

DISCUSSION PAPER SERIES

IZA DP No. 14116

**COVID-19 Severity: A New Approach to
Quantifying Global Cases and Deaths**

Daniel L. Millimet
Christopher F. Parmeter

FEBRUARY 2021

DISCUSSION PAPER SERIES

IZA DP No. 14116

COVID-19 Severity: A New Approach to Quantifying Global Cases and Deaths

Daniel L. Millimet

Southern Methodist University and IZA

Christopher F. Parmeter

University of Miami

FEBRUARY 2021

Any opinions expressed in this paper are those of the author(s) and not those of IZA. Research published in this series may include views on policy, but IZA takes no institutional policy positions. The IZA research network is committed to the IZA Guiding Principles of Research Integrity.

The IZA Institute of Labor Economics is an independent economic research institute that conducts research in labor economics and offers evidence-based policy advice on labor market issues. Supported by the Deutsche Post Foundation, IZA runs the world's largest network of economists, whose research aims to provide answers to the global labor market challenges of our time. Our key objective is to build bridges between academic research, policymakers and society.

IZA Discussion Papers often represent preliminary work and are circulated to encourage discussion. Citation of such a paper should account for its provisional character. A revised version may be available directly from the author.

ISSN: 2365-9793

IZA – Institute of Labor Economics

Schaumburg-Lippe-Straße 5–9
53113 Bonn, Germany

Phone: +49-228-3894-0
Email: publications@iza.org

www.iza.org

ABSTRACT

COVID-19 Severity: A New Approach to Quantifying Global Cases and Deaths*

Accurate counts of cases and deaths are critical for devising an optimal pandemic response. Yet, as the COVID-19 pandemic has progressed, so too has the recognition that cases and deaths have been underreported, perhaps vastly so. Here, we present an econometric strategy to estimate the true number of COVID-19 cases and deaths for roughly 60 countries from January 1 through November 3, 2020. Specifically, we estimate a 'structural' model based on the workhorse SIR epidemiological model extended to incorporate measurement error. The results indicate significant under-reporting by magnitudes that align with existing research and conjectures by public health experts. While our approach requires some strong assumptions, these assumptions are very different from the equally strong assumptions required by other approaches addressing under-reporting in the assessment of the extent of the pandemic. Thus, we view our approach as a complement to existing methods.

JEL Classification: C18, H12, I18

Keywords: COVID-19, nonclassical measurement error, stochastic frontier analysis

Corresponding author:

Christopher F. Parmeter
Department of Economics
Miami Herbert Business School
University of Miami
Miami, FL
USA
E-mail: cparmeter@bus.miami.edu

* All data and Stata code used in this paper are available upon request. We are grateful for comments from Hao Dong and Alecos Papadopoulos.

“If we stop testing right now, we’d have very few cases, if any.”

–President Donald J. Trump on COVID-19 (20 June 2020)

“Political meddling, disorganization and years of neglect of public-health data management mean the country is flying blind.”

–*Nature* on COVID-19 (25 August 2020)

“Many of the infected do not get sick. Many who do are never seen by any health system.”

–*The Economist* on COVID-19 (26 September 2020)

1 Introduction

Efforts by government, media, and public health officials to track the severity and public health impact of COVID-19 in the United States and around the globe have been hampered by a lack of widespread testing, inaccurate tests, reporting lags by government agencies, and inconsistencies in reporting and tracking standards. As a result, the *official* number of COVID-19 cases and deaths likely undercounts the *true* number of cases and deaths, perhaps significantly so. Manski & Molinari (2020, pg. 1) state: “It is well appreciated that accurate characterization of the time path of the coronavirus pandemic has been hampered by a serious problem of missing data.” To estimate the magnitude of this missing data problem, we use data from 63 countries over the period from January 1 to November 3, 2020, a ‘structural’ model based on the workhorse Susceptible-Infected-Removed (SIR) epidemiological model extended to incorporate missing data, and the econometric methodology explored in Millimet & Parmeter (2020) to account for one-sided (nonclassical) measurement error.

In addition to yielding insights into the determinants of cases and deaths, our approach also generates estimates for the true number of cases and deaths due to COVID-19 across the countries in our sample. We estimate the true number of cases to be two to nine times higher than official reports. In terms of deaths, we estimate the true number to be 1.6 to 3.0 times higher than official reports. Over our entire sample, the case fatality rate – observed deaths divided by observed cases – is 2.6%. The infectious fatality rate – estimated deaths divided by estimated cases – ranges from 0.9% to 2.1%. The fact that our estimates of the infectious fatality rate are below the case fatality rate results from our estimate of more missing cases than deaths.

Accurate information on the count of cases and deaths is critical for several reasons. First, under-reporting of cases and deaths inhibits scientific efforts to understand the SARS-CoV-2 virus that causes COVID-19. Correct estimation of rates of transmission, factors affecting transmission, fatality rates, etc. are made all the more difficult without knowledge of the true number of cases and fatalities. As noted in Korolev (2020, pg. 3), “...if one does not take under-reporting into account and estimates R_0 from the

confirmed cases data, assuming that all cases are reported, the estimate of R_0 will be biased downward.”¹ Second, inaccurate information, particularly under-reporting, may inhibit public and political support for warranted responses such as expansions of hospitals, investments in medical equipment, mask mandates, and lockdowns (Depalo 2021, Hortaçsu et al. 2020). Knowledge of undocumented cases is also necessary to assess the risk of infection by the healthy population. As a result, Manski & Molinari (2020), Stock (2020) and others have called for random testing to determine the size of the population of asymptomatic individuals.² Third, underreporting of cases can be fatal. Missing cases precludes complete contact tracing, which in turn leads to greater spread and death (Fetzer & Graeber 2020). Finally, undercounting may lead to sub-optimal government fiscal responses, such as business loans and expanded unemployment insurance, and decisions regarding school closures.

Owing to the importance of accurate information, official figures on cases and deaths have come under increasing scrutiny in the United States and abroad. As recently as June 2020 at least 28 states were not following US Centers for Disease Control and Prevention (CDC) reporting guidelines. While CDC guidelines are voluntary, “states not reporting probable cases likely undercount the number of people infected and make it difficult for officials to get the true picture of where the nation stands in the midst of a pandemic that has rocked almost every aspect of life.”³ Moreover, early testing in the pandemic relied on less than fully accurate nasal swab tests (Manski & Molinari 2020, Reese et al. 2020); recent antibody tests performed in the US suggest that “a good rough estimate now” of the number of missed cases “is 10 to 1.”⁴ However, a mere few days later the CDC reported that the true number of cases “could be up to 24 times higher than reported.”⁵ Anecdotal evidence of under-reporting is also rampant. In Houston some hospitals stopped updating their data once they reached full capacity, “rattling policymakers and residents.”⁶ Government officials in Florida came under fire in May when the data scientist responsible for publishing the state’s data on COVID-19 cases and deaths was terminated.⁷ Finally, a recent article reports that US deaths officially attributed to Alzheimer’s disease and dementia show “how the coronavirus pandemic has exacted a higher fatality toll than official numbers have shown.”⁸

Outside the US, data concerns are no less common. Many “experts . . . fear substantial under-reporting” globally.⁹ Russia, initially claiming its low death toll was a “miracle,” subsequently revised its official number of deaths in April upward by a factor of two.¹⁰ However, some speculate that “about 70 percent of coronavirus-related deaths have not been reported in Moscow and about 80 percent in the country’s

¹As discussed later, R_0 is the reproduction number, or the expected number of secondary cases spawning from each infected individual.

²This is consistent with the approach in Iceland, where the government had randomly tested 26,762 per million inhabitants by March 21, 2020, a number much higher than anywhere else in the world at the time. See <https://www.government.is/news/article/?newsid=f96a270c-66e8-11ea-945f-005056bc4d74>.

³See <https://www.cnn.com/2020/06/09/health/us-coronavirus-tuesday/index.html>.

⁴See <https://www.cnn.com/2020/06/25/health/us-coronavirus-thursday/index.html>.

⁵See <https://www.cnn.com/2020/06/29/health/us-coronavirus-monday/index.html>.

⁶See <https://www.houstonchronicle.com/news/houston-texas/houston/article/Houston-hospitals-hit-100-base-ICU-capacity-15372256.php>.

⁷See <https://www.cnn.com/2020/05/20/us/florida-georgia-covid-19-test-data/index.html>. Since then, Rebekah Jones publishes data on her own, providing numbers above official state figures. See <https://www.washingtonpost.com/nation/2020/06/12/coronavirus-live-updates-us/>. We note here that her numbers also include results from antibody tests, the reliability of which are suspect.

⁸See <https://www.wsj.com/articles/coronavirus-pandemic-led-to-surge-in-alzheimers-deaths-11593345601>.

⁹See <https://www.reuters.com/article/us-health-coronavirus-global-cases/global-coronavirus-cases-surpass-3-5-million-amid-under-reporting-fears-idUSKBN22G00Z>.

¹⁰See <https://www.nytimes.com/2020/05/29/world/coronavirus-update.html>.

regions.”¹¹ While the official number of cases in Brazil recently topped six million, the reported cases are viewed as a vast undercount “because there is under-reporting of a magnitude of five to 10 times.”¹² On July 18, 2020 the president of Iran suggested that 25 million residents have been infected, “nearly a third of the population and massively higher than the official number of COVID-19 cases.”¹³ A recent study in Italy documented evidence that residents in Italy were infected as far back as September 2019 even though the first official case was not recorded until February 2020.¹⁴

Of course, these measurement issues should not be surprising as counting COVID-19 cases and deaths is fraught with difficulty. To begin, a shortage of information and tests during the early stages of the pandemic may have led to many cases and/or deaths being misdiagnosed. Moreover, many deaths due to COVID-19 are not reported as such if individuals were not previously diagnosed with the disease through a positive test. Reporting of deaths is also inconsistent over time and across countries (Flaxman et al. 2020). In the US, for example, doctors and coroners have broad discretion in the determination of cause of death which can lead to inconsistencies.¹⁵ That such discretion has led to under-reporting is borne out by a few instances of *ad hoc* corrections that have occurred. For instance, in early April, New York City experienced a one day increase in COVID-19 deaths of over 3,700 as they retroactively counted past deaths that were likely from COVID-19.¹⁶ New Jersey reported a one day jump of over 1,900 deaths due to COVID-19 toward the end of June, again due to retroactive changes in how deaths were classified.

Today, current case counts remain of questionable accuracy due, in part, to a lack of universal or even randomized testing. It is now well known that a significant number of the infected are asymptomatic, thereby evading official counts in the absence of such testing protocols. Moreover, there is concern in many countries, including the US, that political corruption plays a role in under-reporting.

To overcome this missing data problem, researchers have pursued several approaches to date which we discuss these in detail in the next section. In this paper, we propose an alternative method to assess undercounting based on an extended version of the SIR epidemiological model and the econometric methodology discussed in Millimet & Parmeter (2020). Specifically, Millimet & Parmeter (2020) propose using stochastic frontier analysis (SFA) to estimate models where the outcome is believed to suffer from one-sided or skewed measurement error. Given the overwhelming evidence suggesting that both COVID-19 cases and deaths are undercounted, SFA offers a convenient framework to assess the true extent of the pandemic. See Badunenko et al. (2012) for a recent investigation of SFA.

Estimating stochastic frontier models on weekly data from 63 countries under varying distributional assumptions concerning the measurement error, we reach several striking conclusions. First, we find evidence of significant under-reporting, with our preferred estimates suggesting that the true case (death) count to be roughly nine (two) times higher than official reports. Second, we obtain an infectious fatality rate less than 1%, well below the observed case fatality rate. Third, consistent with conjectures in the epidemiological literature, we find no evidence that the extent of under-reporting is waning. Third, we

¹¹See <https://www.nytimes.com/2020/05/11/world/europe/coronavirus-deaths-moscow.html>.

¹²See <https://www.cnn.com/2020/06/20/brazil-passes-1-million-coronavirus-cases-with-no-end-in-sight.html>.

¹³See <https://www.reuters.com/article/us-health-coronavirus-iran-idUSKCN24K0E3>.

¹⁴See <https://www.reuters.com/article/us-health-coronavirus-italy-timing/coronavirus-emerged-in-italy-earlier-than-thought-italian-study-shows-idUSKBN27VOKF>.

¹⁵See <https://www.scientificamerican.com/article/how-covid-19-deaths-are-counted1/>.

¹⁶See <https://abcnews.go.com/Health/coronavirus-updates-us-navy-battles-growing-outbreak-hospital/story?id=70134122>.

document a robust positive (negative) association between testing and the number of cases (deaths). Finally, we generally find a negative association between the stringency of non-pharmaceutical interventions (NPIs) and cases and deaths. However, this association varies over time and is sensitive to assumptions concerning the nature of the under-reporting.

We are fully aware that no statistical approach to estimating the true number of cases and deaths is beyond reproach. As Manski & Molinari (2020, pg. 12) state, instead of relying on strong assumptions, “a more satisfactory approach to increase knowledge of the infection rate is to obtain better data.” In lieu of better data, SFA is a convenient tool that provides a valuable complement to existing research. While one can certainly criticize the reliance of SFA on distributional assumptions, we provide a range of estimates by employing various assumptions on the measurement error process. This range is broadly consistent with other estimates of under-reporting of cases and deaths. Thus, even with the adherence to parametric distributional assumptions, our findings are both timely and representative. Finally, as detailed in the next section, alternatives to SFA either rely on alternative sets of strong assumptions or rely on weaker assumptions at the expense of point identification. Moreover, these alternatives are often country- or time-specific. Our analysis should be viewed as adding to the totality of scientific evidence using assumptions that are likely orthogonal to those employed by alternative methodologies.

The remainder of the paper proceeds as follows. Section 2 provides a brief literature review. Section 3 outlines the model and econometric framework and discusses the data. Section 4 presents the results. Section 5 concludes.

2 Literature Review

While there is ample evidence of under-reporting of COVID-19 cases and deaths appearing in various media outlets, the scientific research is limited. The most common approach is to focus on fatalities and quantify the amount of missing data via excess mortality. Measures of excess mortality are computed by comparing deaths in 2020 to the number of deaths over the same time period in previous years. This count of ‘excess’ deaths is then compared to official death tolls from COVID-19. Although straightforward, this approach is not without criticism. First, and most importantly, data on all-cause mortality are not available for most countries, let alone data on deaths by category (such as pneumonia and influenza). Moreover, even when such data are available, reporting standards are inconsistent across countries. The *Financial Times* has been most diligent about reporting excess mortality, but these data are only available for 21 countries.¹⁷

Second, conclusions based on excess mortality potentially confound true deaths with other changes as a result of the pandemic. For example, Oguzoglu (2020) reports a reduction in traffic fatalities across 31 metropolitan areas in Turkey due to implementation of various social distancing measures. Dang & Trinh (2020) documents a significant reduction of air pollution in Vietnam due to the pandemic. Reductions in elective health procedures or changes in usage of preventative medical services may also affect mortality during the pandemic but not be directly attributable to COVID-19. Finally, excess mortality is not particularly useful in predicting the true number of cases absent knowledge of the true fatality rate.

Despite these shortcomings, excess mortality serves as a useful benchmark for gauging the extent of

¹⁷See <https://www.ft.com/content/6bd88b7d-3386-4543-b2e9-0d5c6fac846c>.

undercounting of deaths. For instance, Weinberger et al. (2020) use excess deaths related to pneumonia and influenza to estimate the true death toll from COVID-19 in the US early in the pandemic. Their approach fits a Poisson regression over five years of weekly data and then predicts deaths that should have arisen in a given period. Comparing predicted and reported deaths, the authors find roughly 2.6 predicted deaths per officially reported death; this is referred to as the multiplication factor (MF) for deaths. Similarly, the National Statistical Agency of Italy used data on excess deaths through March 31 and reported a MF of 1.8 (Backhaus 2020). More recently, the CDC reported a MF of 1.4 based on excess mortality in the US.¹⁸

Overcoming the missing data problem for the number of infections has a lengthy history in the infectious disease and epidemiological literatures; see Gibbons et al. (2014) for a recent discussion. Approaches are often cast in terms of quantifying underestimation (UE) of a particular disease and decomposing UE into under-reporting (UR) and under-ascertainment (UA). UE is defined as the number of cases missed by official counts and arises from both UR and UA. UR is defined as cases that are missed despite individuals seeking treatment. This could arise either unintentionally (due to misdiagnosis) or intentionally (due to political corruption). UA is defined as cases that are missed because infected individuals remain outside surveillance systems either due to being asymptomatic or not seeking treatment. The objective is to estimate UR and UA, and hence UE, to calculate a MF for cases (i.e., the ratio between the true and reported number of cases).

The standard suite of methods and study designs which can be used to determine the extent of UR and UA include: community-based studies (CBS)¹⁹; serological surveys (which measure sero-incidence or sero-prevalence); returning traveler studies (RTS); and capture-recapture studies (CRS). Upon estimation of UE, researchers can derive country-specific MFs. Typically, researchers rely on simulation methods or national data coupled with CBS or CRS. For example, during the H1N1 outbreak, Reed et al. (2009) estimated MFs on the order of 79, implying a median estimate of nearly three million H1N1 infections even though at the time of their study there were only 43,677 laboratory confirmed cases.²⁰ Reese et al. (2020) follow the same strategy as in Reed et al. (2009) to estimate the number of COVID-19 cases in the US through the end of September. The authors estimate roughly 52.9 million cases. Given a reported count of 6.9 million cases, this yields an MF of 7.7.

The three studies most closely related to ours are Li et al. (2020), Flaxman et al. (2020), and Hortaçsu et al. (2020). Li et al. (2020) study undocumented COVID-19 infections in China for the weeks bracketing the closure of Wuhan. They use an iterated filter-ensemble adjustment Kalman filter framework to estimate the trajectories of four key variables: the susceptible population, the exposed population, and both documented and undocumented infections. Their results suggest that 86% of infections went undocumented (a MF over 7). Flaxman et al. (2020) chart the course of the COVID-19 epidemic by back-calculating infections from observed deaths across eleven European countries. They introduce a Bayesian mechanistic model to connect the infection cycle to observed deaths. The model is then used to infer the total population infected and the reproduction number, R_0 , over time in each country. For the countries considered,

¹⁸See <https://www.ft.com/content/752384ef-fc13-3e46-a76d-c4ef5dc5444b>.

¹⁹Gibbons et al. (2014, pg. 147) state: “CBS can take many forms but generally involve active searching within the community for disease episodes, pathogen carriage or infection, with questionnaire-based data acquisition often accompanied by biological sampling. Active searching can be conducted face-to-face, by telephone, internet or post, with several possible study designs e.g. based on probability samples, prospective or retrospective cohorts, population cross-sections, involving representative samples of the whole population or certain interest or high-risk groups only.

²⁰Additionally, there were 302 deaths from H1N1 reported at the time of the study by Reed et al. (2009), but their MFs for UR of hospitalizations, coupled with a 6% death rate, suggests that there over 800 deaths from H1N1.

the authors estimate 12 to 15 million COVID-19 cases whereas the official count was roughly one million (a MF of at least 12). Consistent with our approach, Flaxman et al. (2020, pg. 2) conclude that "...there are orders of magnitude fewer infections detected ... than true infections, most likely due to mild and asymptomatic infections as well as limited testing capacity and changes in testing policy."

Finally, Hortaçsu et al. (2020) devise a creative way to estimate a MF for cases in the US based on data on travel patterns. As with our approach, their strategy entails a number of strong assumptions. Moreover, their approach is perhaps limited in its generalizability to other countries and later periods of the pandemic due to data demands and the nature of the identifying assumptions. Specifically, their approach assumes that the pandemic originates in an epicenter and spreads to other regions via travelers. Given data on travel patterns, combined with assumptions on selection into travel, the transmission rate, and the infection rate in the epicenter, the authors estimate the expected number of infections outside the epicenter. The ratio of this expectation and the official number of cases yields the MF. In the US very early in the pandemic (through March 16), they obtain a MF between 6 and 24.

Two other studies merit discussion. Depalo (2021) and Manski & Molinari (2020) diverge from the preceding studies in that they consider what can be learned about COVID-19 given missing data under weaker assumptions. As a result, both papers focus on partial identification of the incidence and severity of COVID-19. Depalo (2021) combines incomplete administrative data on excess mortality in Lombardia, Italy with assumptions on excess mortality in unobserved municipalities to partially identify the true number of COVID-19 deaths. The author also uses incomplete data on testing to partially identify the true number of COVID-19 cases. Manski & Molinari (2020) partially identify the infection rate and the infectious fatality rate accounting for uncertainty due to the lack of universal or random testing and the inaccuracy of tests. Unfortunately, with the information available, it is not possible to partially identify MFs from these studies.

Beyond the specific issue of under-reporting of COVID-19 cases and deaths, our approach also yields estimates of the association between NPIs (along with other country-specific attributes such as testing) and COVID-19 cases and deaths. Thus, our study also relates to existing analyses of the efficacy of NPIs. Chudik et al. (2020) extend the SIR model to allow for different degrees of compulsory and voluntary social distancing. Their model is used to study the impact of social distancing on both the spread of COVID-19 and unemployment across Chinese provinces. Noteworthy, the authors specifically account for under-reporting using an assumed MF of 2, which they justify on the basis of data on the number of asymptomatic individuals aboard the Diamond Princess cruise ship. Their model assumes that under-reporting follows a log-normal distribution, which is then used in a nonlinear equation to discern the impact of social distancing on unemployment. Chernozhukov et al. (2020) and Flaxman et al. (2020), similar to Chudik et al. (2020), find that NPIs (stay-at-home orders and business closures, in particular) substantially reduced transmission. Additionally, Chernozhukov et al. (2020) estimate that a mask mandate would have reduced the growth rate of infections by ten percentage points and the the number of deaths by at least 19% early in the pandemic. Lastly, Askitas et al. (2020) exploit both between and within country variation in the type, timing, and level of six different NPIs across 135 countries. The authors finding that a unit increase in the intensity of public events cancellations leads to a 25% decrease in the number of new infections of COVID-19.

3 Empirics

3.1 An Epidemiological Model with Measurement Error

We begin with the classic SIR model (Kermack & McKendrick 1927). As stated in Avery et al. (2020, pg. 80), the SIR model “serves as the basis of much of modern epidemiology of infectious disease, both theoretical and empirical.” However, we extend the model to incorporate missing data. Broadly, the SIR model posits that the population of country i at any time t is divided into three distinct compartments: susceptible, S^* , infected, I^* , and removed, R^* . Thus,

$$S_{it}^* + I_{it}^* + R_{it}^* = N_{it}, \quad (1)$$

where N_{it} is the overall population.

The change in the number of susceptibles at time t is given by

$$\frac{dS_{it}^*}{dt} = -\beta_{it}I_{it}^*S_{it}^*, \quad (2)$$

where β_{it} is the number of contacts that occur in country i in period t between infected and susceptible individuals. As the pool of infected individuals increases, the number of susceptible individuals decreases; newly infected individuals are reclassified from S_{it}^* to I_{it}^* .

The change in the number of infected depends on the number of susceptibles that become infected and the number of infected that are removed. Removal can happen either through recovery or death.²¹ The change in the number of infected at time t is given by

$$\frac{dI_{it}^*}{dt} = \beta_{it}I_{it}^*S_{it}^* - (\gamma_{1it} + \gamma_{2it})I_{it}^*, \quad (3)$$

where γ_{1it} is the recovery rate and γ_{2it} is the fatality rate. The reproduction number, R_0 , is $R_{0it} = \beta_{it}/(\gamma_{1it} + \gamma_{2it})$; Atkeson (2020) refers to R_0 as the normalized transmission rate. Our modeling of the reproduction rate as country- and time-specific follows from the fact that individual and government behavior evolves over the course of the pandemic (Avery et al. 2020). Finally, the change in the number of recovered and dead at time t is given by

$$\frac{dR_{1it}^*}{dt} = \gamma_{1it}I_{it}^* \quad (4)$$

$$\frac{dR_{2it}^*}{dt} = \gamma_{2it}I_{it}^*, \quad (5)$$

respectively.

Equation (3) gives the change in the infected population. The number of new cases at time t , Y_{it}^* , is given by the first term,

$$Y_{it}^* \equiv \beta_{it}I_{it}^*S_{it}^*. \quad (6)$$

In the presence of measurement error, we model the relationship between the true number of new cases,

²¹This is sometimes referred to as a Susceptible-Infected-Recovered-Dead (SIRD) model. See, e.g., Chernozhukov et al. (2020).

Y^* , and the reported number of cases, Y , as

$$Y_{it}^* = Y_{it} \exp(u_{it}^Y), \quad (7)$$

where Y_{it}^*/Y_{it} is the MF for cases. If $u_{it}^Y \in \mathcal{R}^+$, then $Y_{it} < Y_{it}^*$, MF is greater than one, and new cases at time t are under-reported. Modeling measurement error in this way is similar to Atkeson (2020); however, Atkeson (2020) assumes u_{it}^Y is constant over time. Moreover, Atkeson (2020) does not take a stance on the sign of u_{it}^Y . As discussed above, there is widespread belief that reported cases of COVID-19 are under-reported. Nonetheless, our analysis can be viewed as a test of this (as discussed below in footnote 24).

Substituting (7) into (6), taking logarithms, and rearranging yields

$$\ln(Y_{it}) \equiv \ln(\beta_{it}) + \ln(I_{it}^*) + \ln(S_{it}^*) - u_{it}^Y. \quad (8)$$

While S_{it}^* and I_{it}^* are unobserved, equation (1) implies the following relationship

$$\begin{aligned} \ln(N_{it}) &= \ln(S_{it}^* + I_{it}^* + R_{it}^*) \\ &= \ln \left[S_{it}^* \left(1 + \frac{I_{it}^* + R_{it}^*}{S_{it}^*} \right) \right] \\ &= \ln(S_{it}^*) + \ln \left(1 + \frac{I_{it}^* + R_{it}^*}{S_{it}^*} \right) + \ln(I_{it}^*) - \ln(I_{it}^*) \\ &= \ln(S_{it}^*) + \ln(I_{it}^*) + \ln \left(\frac{N_{it}}{S_{it}^* I_{it}^*} \right) \\ &= \ln(S_{it}^*) + \ln(I_{it}^*) + \tilde{v}_{it}, \end{aligned} \quad (9)$$

where $\tilde{v}_{it} \in \mathcal{R}$.²² Substituting (9) into (8) yields

$$\ln(Y_{it}) \equiv \ln(\beta_{it}) + \ln(N_{it}) - u_{it}^Y + v_{it}, \quad (10)$$

where $v_{it} = -\tilde{v}_{it}$.

Finally, we assume that β_{it} can be modeled partially in a deterministic fashion. Specifically, let

$$\ln(\beta_{it}) = X_{it} \beta_X + v_{it}^\beta, \quad (11)$$

where $v_{it}^\beta \in \mathcal{R}$. X includes geographic, demographic, and political characteristics of country i , as well as variables measuring the extent of COVID-19 testing being performed and the strength of NPIs taken by the country prior to t . We also include region-specific time trends in β_{it} and we allow the marginal effects of testing and NPIs to vary over time. We do so to avoid the critique levied in Avery et al. (2020, pg. 89) that ‘‘tightly parameterized models lack the flexibility to respond to qualitative changes in disease behavior that are inconsistent with earlier apparent patterns’’ such as ‘‘repeated changes in the rate of spread due to changing regulations, changing public perception, and ‘quarantine fatigue.’’’

Our setup is similar in spirit to the random walk approach used in Arroyo-Marioli et al. (2020). While

²²Setting $R_{it}^* = 0$ for simplicity and noting that $S_{it}^* \gg 0$, then $N_{it} > (<) S_{it}^* I_{it}^*$ if $I_{it}^* < (>) 1$. Because I_{it}^* (as well as S_{it}^* and N_{it}) can be measured in, say, population in millions, it may be greater than or less one. Thus, \tilde{v}_{it} is a two-sided error term.

Arroyo-Marioli et al. (2020) model β_{it} in levels as a random walk with an additive error, we model β_{it} in levels as a deterministic function with a proportional error. Thus, taking logarithms in our model produces an additive error. Incorporating this, our estimating equation becomes

$$\ln(Y_{it}) \equiv X_{it}\beta_X + \beta_N \ln(N_{it}) - u_{it}^Y + v_{it}^Y, \quad (12)$$

where $v_{it}^Y \equiv v_{it} + v_{it}^\beta$.²³

Turning to deaths, equation (5) gives the change in deaths. Thus, the number of new deaths at time t , D_{it}^* , is given by

$$D_{it}^* \equiv \gamma_{2it} I_{it}^*. \quad (13)$$

In the presence of measurement error, we model the relationship between the true number of new deaths, D^* , and the reported number of new deaths, D , as

$$D_{it}^* = D_{it} \exp(u_{it}^D), \quad (14)$$

where D_{it}^*/D_{it} is the MF for deaths. If $u_{it}^D \in \mathcal{R}^+$, then $D_{it} < D_{it}^*$, the MF is greater than one, and new deaths at time t are under-reported. Substituting (14) into (13), taking logarithms, and rearranging yields

$$\ln(D_{it}) \equiv \ln(\gamma_{2it}) + \ln(I_{it}^*) - u_{it}^D. \quad (15)$$

As before, assume that γ_{2it} can be modeled partially in a deterministic fashion. Specifically, let

$$\ln(\gamma_{2it}) = X_{it}\gamma_X + v_{it}^\gamma, \quad (16)$$

where $v_{it}^\gamma \in \mathcal{R}$. Substituting this into (15) and replacing I^* with N produces our estimating equation

$$\ln(D_{it}) \equiv X_{it}\gamma_X + \gamma_N \ln(N_{it}) - u_{it}^D + v_{it}^D, \quad (17)$$

where $v_{it}^D \equiv v_{it}^\gamma + \ln(I_{it}^*) - \gamma_N \ln(N_{it}) = v_{it}^\gamma - \tilde{v}_{it} - \ln(S_{it}^*) - (1 - \gamma_N) \ln(N_{it})$.

3.2 Estimation

Our objective is to estimate equations (12) and (17). In addition to obtaining coefficient estimates, we also wish to obtain estimates of u_{it}^Y and u_{it}^D to recover estimates of the actual number of cases, Y_{it}^* , and deaths, D_{it}^* . Fortunately, as discussed in Millimet & Parmeter (2020), the estimating equations above have a parallel structure to stochastic frontier models if one is willing to assume that the measurement errors, u_{it}^Y and u_{it}^D , are one-sided (Aigner et al. 1977).²⁴ Thus, Millimet & Parmeter (2020) show via simulations

²³Note, if $S_{it}^*, I_{it}^* \gg 0$, then v_{it} will be skewed in the positive direction. Assuming v_{it}^β is symmetrically distributed around zero, this will make our estimates of under-reporting a lower bound.

²⁴Note, the assumption that the measurement errors are one-sided (i.e., cases and deaths are under-reported) is not particularly controversial. For example, as discussed in Manski & Molinari (2020), self-selection into testing combined with the asymmetric inaccuracy of nasal swab tests (with very few false positives, but many false negatives) leads to undercounting. Backhaus (2020), Hortaçsu et al. (2020), and Reese et al. (2020) emphasize the problem of missing data on asymptomatic individuals and the lack of (accurate) testing. Nonetheless, this is a ‘testable’ assumption in the sense that identification in the stochastic frontier model requires the composite error term to be negatively skewed. If the measurement errors are not one-sided (or at least strongly skewed toward negative values), then identification will fail.

and several empirical replications that SFA can be a valuable tool to address one-sided measurement error.

To proceed, we make distributional assumptions for v_{it}^q and u_{it}^q , $q \in \{Y, D\}$, and estimate the models by maximum likelihood where the dependent variables are transformed using the inverse hyperbolic sine transformation (IHS) to account for zeros (Askatas et al. 2020, Bellemare & Wichman 2020, Goolsbee & Syverson 2020).²⁵ To assess sensitivity, we consider four sets of distributional assumptions. First, we assume that $v_{it}^q \stackrel{\text{iid}}{\sim} N(0, \sigma_{v^q}^2)$ and $u_{it}^q \stackrel{\text{iid}}{\sim} N^+(0, \sigma_{u^q}^2)$. This gives rise to the following log-likelihood function

$$\ln L = \sum_{i=1}^N \sum_{t=1}^{T_i} \left\{ -\ln \sigma_{\varepsilon^q} + \ln \Phi \left[-\frac{\varepsilon_{it}^q \left(\frac{\sigma_{u^q}}{\sigma_{v^q}} \right)}{\sigma_{\varepsilon^q}} \right] - \frac{(\varepsilon_{it}^q)^2}{2\sigma_{\varepsilon^q}^2} \right\}, \quad q \in \{Y, D\} \quad (18)$$

where $\varepsilon_{it}^q \equiv v_{it}^q - u_{it}^q$ is the composite error term, $\Phi(\cdot)$ is the standard normal cumulative distribution function, and $\sigma_{\varepsilon^q}^2 = \sigma_{v^q}^2 + \sigma_{u^q}^2$ (Parmeter & Kumbhakar 2014).

Second, we assume that $v_{it}^q \stackrel{\text{iid}}{\sim} N(0, \sigma_{v^q}^2)$ and $u_{it}^q \stackrel{\text{iid}}{\sim} \text{Exp}(\lambda^q)$ (Meeusen & van den Broeck 1977). The exponential distribution has several diagnostic advantages over the half-normal as it allows for a greater range of both skewness and kurtosis of the composite error, ε_{it}^q , providing greater flexibility to match its shape (Papadopoulos & Parmeter 2020). The log-likelihood function is given by

$$\ln L = \sum_{i=1}^N \sum_{t=1}^{T_i} \left\{ -\ln \sigma_{u^q} + \frac{\sigma_{v^q}^2}{2\sigma_{u^q}^2} + \ln \Phi \left[-\frac{\varepsilon_{it}^q + \left(\frac{\sigma_{v^q}^2}{\sigma_{u^q}} \right)}{\sigma_{v^q}} \right] + \frac{\varepsilon_{it}^q}{\sigma_{u^q}} \right\}, \quad q \in \{Y, D\}. \quad (19)$$

Third, we relax the independence assumption by estimating a stochastic frontier model with time invariant measurement error, u_i^q (Pitt & Lee 1981). Specifically, $\varepsilon_{it}^q = v_{it}^q - u_i^q$, where $v_{it}^q \stackrel{\text{iid}}{\sim} N(0, \sigma_{v^q}^2)$ and $u_i^q \stackrel{\text{iid}}{\sim} N^+(0, \sigma_{u^q}^2)$. The assumption of time invariant measurement error is restrictive, but relaxes the assumption of independent measurement errors within a country. Moreover, it may be a reasonable approximation since the dependent variables are transformed using the IHS. As such, a time invariant measurement error implies a constant percentage of under-reporting. For cases, this may be plausible given that a constant fraction of infected are likely to be asymptomatic. It is also consistent with the claim in Avery et al. (2020, pg. 89) that “observation error can rise as larger swaths of the population are infected and contact tracing becomes less reliable.” For deaths, it may be plausible as well given that reporting practices for cause of death are likely fixed during the initial waves of the pandemic.

That said, it is also possible that the proportion of missing data may vary over time. Murray (2020, pg. 110) states: “For diseases with more common mild and asymptomatic cases ... the completeness of the data can vary in complex ways over time.” Thus, in our final specification, we relax the assumption of time invariant measurement error assumption and estimate a time-varying decay model. In this case, $\varepsilon_{it}^q = v_{it}^q - u_{it}^q$, where $v_{it}^q \stackrel{\text{iid}}{\sim} N(0, \sigma_{v^q}^2)$, $u_{it}^q = \exp[-\eta^q(t - T_i)] u_i^q$, and $u_i^q \stackrel{\text{iid}}{\sim} N^+(0, \sigma_{u^q}^2)$. The sign of η determines whether the extent of under-reporting is increasing or decreasing over time; $\eta < 0$ implies that it is increasing over time while $\eta > 0$ implies the reverse. The log-likelihood function is given by

²⁵Importantly, the coefficient estimates are consistent regardless of the distributional assumptions (Papadopoulos & Parmeter 2020). However, estimates of actual cases and deaths may be sensitive to the distributional assumptions. All models are estimated in `Stata` using `frontier` or `xtfrontier`.

$$\ln L = \sum_{i=1}^N \left\{ \ln \Phi \left(\frac{\mu_{i*}^q}{\sigma_*^q} \right) + \frac{1}{2} \ln (\sigma_*^q)^2 - \frac{1}{2} \left[\frac{1}{\sigma_{v^q}^2} \sum_{t=1}^{T_i} (\varepsilon_{it}^q)^2 - \left(\frac{\mu_{i*}^q}{\sigma_*^q} \right)^2 \right] - T_i \ln (\sigma_{v^q}) - \ln (\sigma_{u^q}) \right\}, \quad q \in \{Y, D\} \quad (20)$$

where

$$\begin{aligned} \eta_{it}^q &= \exp[-\eta^q (t - T_i)] \\ \mu_{i*}^q &= \frac{-\sigma_{u^q}^2 \sum_{t=1}^{T_i} \eta_{it}^q \varepsilon_{it}^q}{\sigma_{v^q}^2 + \sigma_{u^q}^2 \sum_{t=1}^{T_i} (\eta_{it}^q)^2} \\ \sigma_*^q &= \frac{\sigma_{v^q}^2 \sigma_{u^q}^2}{\sigma_{v^q}^2 + \sigma_{u^q}^2 \sum_{t=1}^{T_i} (\eta_{it}^q)^2}. \end{aligned}$$

The log-likelihood of the time invariant model is obtained by maximizing (20) imposing the constraint $\eta^q = 0$.²⁶

Upon estimation of the model, the level of under-reporting, u_{it}^q , can be estimated (Jondrow et al. 1982). This is calculated from the conditional expectation of the one-sided error given the composite residual. In the case of the time invariant and time-varying decay models, this is given by

$$E[u_i^q | \varepsilon_i^q] = \mu_{i*}^q + \sigma_*^q \left[\frac{\phi(-\omega_{i*}^q)}{1 - \Phi(-\omega_{i*}^q)} \right], \quad (21)$$

where $\omega_{i*}^q = \mu_{i*}^q / \sigma_*^q$.

There certainly exist alternative approaches we could deploy given the panel setup; see Parmeter & Kumbhakar (2014) for a thorough review. However, our approach is consistent with several recent COVID-19 studies. Li & Linton (2020) estimate linear regression models for the logarithm of daily cases and deaths to forecast future trajectories. Chernozhukov et al. (2020) estimate linear regression models for the growth rate of weekly cases and deaths in the US to assess the impact of NPIs and behavioral responses. Weinberger et al. (2020) examine pneumonia and influenza deaths in order to assess excess mortality using a Poisson regression framework, treating deaths as a count variable. Teixeira da Silva & Tsigaris (2020) estimate cross-country linear regression models to explore determinants of the case fatality rate.

Although continuing in this line of analysis, our approach is not meant to displace alternative, more traditional epidemiological approaches, nor alternative structural approaches such as in Hortaçsu et al. (2020), but to complement them. Our approach offers numerous advantages. First, it provides estimates under alternative assumptions than existing methods designed to correct for under-reporting. Second, our method is estimable across a large range of countries. Finally, our approach could prove especially useful early in pandemics when epidemiological approaches based on community-based or serological surveys take for the spread of the diseases to reveal itself.

²⁶The likelihood function in (18) is identical to 20 with $\eta^q = 0$ and $T_i = 1 \forall i$.

3.3 Data

Data on official reports of daily COVID-19 cases and deaths are obtained from *Our World in Data*.²⁷ We utilize data from 1 January 2020 through 3 November 2020 (i.e., the first 44 weeks of 2020). We restrict our sample to countries observed in every week. This leads to a sample of 63 countries which are listed in Table 1. In our analysis, we further restrict the sample along two dimensions. In the models for both cases and deaths, we restrict the sample to weeks following the first week with at least five newly reported cases. In the models for deaths, we further restrict the sample to weeks following the first week with at least ten newly reported deaths.²⁸ Our dependent variables are new cases and deaths aggregated to the weekly level.

Control variables include population, population density, median age, the percent of the population aged 65 and above, diabetes prevalence, and per capita Gross Domestic Product. These variables come from the same source as the COVID-19 data. Sá (2020) uses similar controls to discern determinants of reported cases and deaths in England and Wales through May 2020. In addition, we also control for lagged weekly tests obtained from the same source.²⁹ We include Transparency International’s 2019 Corruption Perception Index as a country-level measure of corruption.³⁰ Finally, we include a time-varying index of the stringency of NPIs undertaken in each country. The index is taken from the Oxford COVID-19 Government Response Tracker (OxCGRT), varies between 0 and 100, and varies over time (Hale et al. 2020).³¹ Given that the estimated incubation period for COVID-19 has been reported to be between 14 and 21 days, and deaths likely occur after a further delay, we use lags of the NPI stringency index. When modeling new cases, we consider the average of the index computed over the third and fourth lags. When modeling new deaths, we use the average of the index computed over the fifth and sixth lags. Excluding countries with missing covariate data reduces our sample to 61 countries when assessing cases and 56 countries when analyzing deaths.

All models include region fixed effects (East Asia and the Pacific, Europe and Central Asia, Latin America and the Caribbean, Middle East and Africa, and South Asia) and region-specific linear time trends. The time trends are measured relative to time in the sample (i.e. weeks after first week with reported cases or deaths above the threshold), not calendar time. We also interact NPI stringency and testing with a linear (calendar) time trend to allow for changes in the effectiveness of each over time. Finally, we include quadratics for the continuous country characteristics to allow for nonlinear effects.

²⁷Specifically, the data are available at <https://github.com/owid/covid-19-data/tree/master/public/data>.

²⁸These sample restrictions are not strictly necessary. However, the stochastic frontier models can have a difficult time converging otherwise. That said, it is also consistent with the manner in which cases and deaths are reported in the popular press, where countries observed paths are discussed after the country passes an initial milestone.

²⁹Data on new tests are measured in different units across countries (people tested, samples tested, tests conducted, or unclear). To account for this, we include dummy variables for the unit of measurement as well as interactions between these dummy variables and the continuous measure of new tests.

³⁰See <https://www.transparency.org/en/cpi>.

³¹The data are available at <https://www.bsg.ox.ac.uk/research/research-projects/coronavirus-government-response-tracker>. We use the containment and health index.

4 Results

4.1 COVID-19 Cases & Deaths

4.1.1 Stochastic Frontier Models Assuming Independent Measurement Errors

Table 2 presents select coefficient estimates from our specifications assuming independent measurement errors.³² Columns 1 and 2 assume the measurement error is distributed half-normal; columns 3 and 4 assume an exponential distribution. The dependent variable in Columns 1 and 3 is the IHS transformation of weekly cases. The dependent variable in Columns 2 and 4 is the IHS transformation of weekly deaths. In the table we also report the mean of the observation-specific marginal effects of the lagged containment index (along with its standard error and p -value associated with the two-sided test that this effect is zero). Lastly, the final two rows in the table display the cumulative total number of observed and estimated cases and deaths over the sample period. In total, roughly 37.66 million cases have been reported along with about 0.98 million deaths.

Figures 1 and 2 plot the average of the country-specific marginal effects over time for the number of tests performed and NPIs, respectively, to facilitate interpretation of the coefficients. Figure 1 shows a positive association between testing and cases since early April. There is a consistently negative association between testing and deaths (when tests are measured in clearly defined units). Moreover, as the marginal effects represent elasticities, the associations are significant in magnitude. Although one should be cautious giving this a causal interpretation, it is nonetheless comforting. It is also comforting that the distributional assumption concerning the measurement error has little impact on the estimates.

Figure 2 reveals a volatile association between NPIs and cases and deaths, although the time pattern is similar across the two outcomes and invariant to the distributional assumptions considered. For both cases and deaths, the association between NPIs and cases and deaths is most negative during Summer 2020. From April through July, NPIs are associated with fewer cases and deaths. However, perhaps due to pandemic fatigue, this association falls to zero and even becomes positive for cases in Fall 2020. To interpret the magnitude of the association, recall that the containment index measuring NPIs ranges from 0 to 100 with a mean close to 50 and a standard deviation of roughly 25. Thus, a one standard deviation increase in this index is associated with a decline in deaths of roughly 40% ($\exp(-0.02 * 25) - 1 = -0.4$) during the summer. This is substantial, consistent with Chernozhukov et al. (2020).³³

Turning to the issue of under-reporting for cases, we estimate a MF of 2.9 (2.0) when the measurement error is assumed to be distributed half-normal (exponential). Given the ranges discussed in Section 2, this is on the low end. Hortaçsu et al. (2020) estimate a MF ranging from 6 to 24, Li et al. (2020) estimate a MF of at least 7, Flaxman et al. (2020) estimate a MF of at least 12, and Reese et al. (2020) estimate an MF of nearly 8. However, our MF is consistent with the argument put forth in Chudik et al. (2020). Needing to choose a MF to calibrate their model, the authors note that of the 3,711 passengers and crew on board the Diamond Princess cruise ship, 712 tested positive for COVID-19. Of these 712 individuals, 331 were asymptomatic at the time of testing.³⁴ Under the assumption that the testing is accurate, this

³²Full results are available upon request.

³³This does contrast with Goolsbee & Syverson (2020) who find that most of the decline in economic activity in the US is attributable to behavioral changes due to fear, not policy changes. However, as stated previously, one should be cautious giving our results a causal interpretation.

³⁴Chudik et al. (2020) report 311, but this number is erroneous.

suggests that the 331 asymptomatic individuals likely would not have been tested – and hence not officially counted – had they not been aboard the Diamond Princess. Thus, the MF is $712/381 \approx 1.9$.³⁵

We find lower levels of under-reporting for deaths. We estimate a MF of 2.2 (1.6) when the measurement error is assumed to be distributed half-normal (exponential). The smaller MF for deaths is not surprising, however, as the under-reporting of COVID-19 cases is most likely due to asymptomatic carriers who never interact with the medical system, whereas under-reported deaths are predominantly due to unintentional or intentional misdiagnosis. Flaxman et al. (2020, pg. 3) state that data on deaths are “... likely to be far more reliable than case data.” Moreover, our estimated MF is in line with figures discussed in Section 2, ranging from 1.4 to 2.6.

For the US we find that through November 3rd the total number of cases was 9,291,234 while the predicted number of cases under the half-normal specification is 24,178,170 (a MF of 2.6) and that for the exponential specification is 17,874,482 (a MF of 1.9). For deaths, again through November 3rd, reported deaths are 231,545, while the half-normal specification predicts deaths at 485,320 (a MF of 2.1) while the exponential specification predicts deaths to be 359,449 (a MF of 1.6).

To visualize the estimated levels of under-reporting, Figures 3 and 4 show graphically the observed and estimated weekly cases and deaths, respectively, for different geographic regions. These figures are obtained directly from the model estimates in Table 2. A few interesting findings stand out. First, the exponential model estimates less under-reporting for all regions for both cases and deaths. Second, in an absolute sense, under-reporting of cases has not waned over time. For the US, Europe and Central Asia, and North America, the absolute amount of under-reported appears to have stabilized in Fall 2020. However, the absolute amount of under-reporting continues to rise in other regions. This is consistent with idea that contact tracing may get exponentially more difficult as more of the population becomes infected (Avery et al. 2020).

Third, whereas the observed data show a decline in new cases for some regions at some points in time, the half-normal model suggests that some of this is illusory. For example, the decline in observed cases in Latin America and the Caribbean starting in late summer is attributable to an increase in under-reporting. Even in Europe and Central Asia during the summer, the modest decline in reported cases is potentially an artifact of under-reporting. Finally, while under-reporting of deaths does not seem to be disappearing either, there is some suggestion that it has declined over time in some regions. For example, for both the United States, Europe and Central Asia, and North America, under-reporting seems most severe early in the pandemic. However, for other regions, most notably Latin America and the Caribbean, South Asia, and East Asia and the Pacific, under-reporting seems to have become worse in Fall 2020.

4.1.2 Stochastic Frontier Models Allowing for Dependence

Table 3 is analogous to Table 2 except the estimates are from our specifications allowing for dependence over time in the measurement errors. Columns 1 and 2 assume the measurement error follows the time-varying decay structure; columns 3 and 4 assume time invariant measurement error. The average of the country-specific marginal effects over time for the number of tests performed and NPIs are shown in Figures

³⁵An alternative figure is available from the testing of all pregnant women delivering infants at the New York-Presbyterian Allen Hospital and Columbia University Irving Medical Center (Sutton et al. 2020). Of the 215 women who delivered, 214 were tested for COVID-19 despite only four mothers displaying symptoms. In addition to these four, another 29 were asymptomatic but tested positive. This suggests a MF of $33/4 \approx 8$, though this is likely not a random sample of the population.

1 and 2, respectively.

Figure 1 shows a positive association between testing and cases since early April in both the time-varying decay and time invariant specifications as in the previous models. If anything, the specifications allowing for dependence find a stronger association between testing and the number of cases as the marginal effects are strictly positive regardless of the units in which the testing data are reported. That said, there is little qualitative difference relative to the prior results obtained assuming independent measurement errors. For deaths there is also little difference compared to the prior results assuming independent measurement errors. Thus, we continue to find a negative association of large magnitude between testing and deaths (when tests are measured in clearly defined units).

Figure 2 shows the marginal effects of NPIs on cases and deaths. Here, the results do differ from the prior specifications assuming independent measurement errors. Specifically, we find a stronger, negative association between NPIs and both cases and deaths when allowing for dependence in the measurement errors. In addition, while the association between NPIs and cases remains positive in the early weeks of the pandemic (as in the prior specifications), the association with deaths is now negative over the entire course of the pandemic to date. Overall, then, the results suggest a stronger, negative association between stringent NPIs and deaths once measurement error is allowed to be temporally dependent.

Turning to the issue of under-reporting for cases, we estimate a MF of 9.0 (3.5) in the time-varying decay (time invariant) specifications. These MFs are notably higher than in the specifications assuming independent measurement errors.³⁶ However, these higher MFs are more in line with alternative estimates presented in Flaxman et al. (2020), Hortaçsu et al. (2020), Li et al. (2020), Reese et al. (2020), and Sutton et al. (2020). For deaths we also find higher levels of under-reporting than in our previous specifications (although still lower than for cases). We estimate a MF of 3.0 (1.9) in the time-varying decay (time invariant) specifications. These figures continue to be in line with figures discussed in Section 2, ranging from 1.4 to 2.6.

To visualize the estimated levels of under-reporting, Figures 5 and 6 show graphically the observed and estimated weekly cases and deaths, respectively, for different geographic regions. As before, these figures are obtained directly from the model estimates in Table 3. A few noteworthy findings emerge. First, while the time-varying decay model predicts more under-reporting overall, there is variation across regions. For example, Figure 5 shows that the time invariant specification yields greater under-reporting for the US and North America, but not in the other regions. Figure 6 shows that the time-varying decay specification yields greater under-reporting in Europe and Central Asia, Latin America and the Caribbean, Middle East and North Africa, and Sub-Saharan Africa. There is little difference between the two specifications for the remaining regions.³⁷

Second, the time-varying decay model indicates that under-reporting for both cases and deaths has increased over time. For both outcomes, the estimate of η is negative and statistically significant ($p < 0.01$).³⁸ This is particularly noticeable for Latin America and the Caribbean, South Asia, East Asia and the Pacific, and Middle East and North Africa. As stated previously, this is consistent with the notion that contact tracing may become exceedingly more difficult as the infection spreads (Avery et al.

³⁶The MF for the US however are roughly similar for the independent error setting.

³⁷South Asia is a bit of an exception. The two specifications yield similar results until later summer, after which the time-varying decay model predicts greater under-reporting.

³⁸For cases, $\hat{\eta} = -0.027$, standard error = 0.003. For deaths, $\hat{\eta} = -0.029$, standard error = 0.003.

2020). Finally, both specifications indicate that Europe and Central Asia are embroiled in a substantial second wave. While both specifications paint a similar picture for the US in terms of cases, there is not a corresponding rise in deaths in the US.

4.2 Country-Specific Multiplication Factors, Infection Rates, Case Fatality Rates, and Infectious Fatality Rates

The model estimates can also be used to assess heterogeneity in pandemic experiences across countries. To start, Table 4 displays country-specific MFs for cases and deaths from each specification over the full sample period. A few key findings stand out. First, rankings of data accuracy across models are highly correlated. The Spearman rank correlations for cases (deaths) all exceed 0.50 (0.43). The MFs from the time-varying decay model are the most divergent from the other specifications; the Spearman rank correlations among the other three specifications all exceed 0.67 (0.64) for cases (deaths). Second, reporting accuracy for the US is roughly middle of the pack. In each of the eight models (two outcomes times four specifications) at least 27 countries have higher MFs than the US. Third, the time-varying decay model produces the greatest heterogeneity in MFs across countries, with some countries having very high MFs.

Figures A1 and A2 in the Appendix plot the weekly MFs for cases and deaths, respectively, for the US and the regions of the world. For cases, the MFs are quite high in the very early stages of the pandemic, as one might expect, for all regions except East Asia and the Pacific and Sub-Saharan Africa. However, the MFs quickly fall and remain relatively constant over the remainder of the sample period. For deaths, a similar pattern emerges, but it is less extreme and less common. Specifically, the MFs are no longer significantly higher early in pandemic for Europe and Central Asia.

Next, we tabulate cumulative infection rates for the countries in our sample. Column 1 in Table 5 shows the observed cumulative infection rate by country, defined as the cumulative number of cases divided by population. The remaining columns report estimated infection rates, defined as the cumulative estimated number of cases divided by population. Note, the ratio of the estimated infection rate to the observed infection rate yields the MFs reported in Table 4. The estimated infection rates for the US and Italy lie within the bounds reported in Manski & Molinari (2020) for New York State, Illinois, and Italy. For the US, our estimated cumulative infection rate ranges from 4.2% to 7.6%, in contrast to the observed rate of 2.8%. Again, this is consistent with the broad findings in the literature that cases in the US are severely under-counted. We also point out that any individual estimate should not be relied on too heavily as for instance both Ecuador and Mexico have predicted cumulative infection rates over 100%. Although not realistic, our estimation procedure does not restrict total cases to be less than the total population.³⁹

Finally, Figure 7 plots the case fatality rate (CFR) and the infectious fatality rate (IFR) over time for the US and the regions of the world. We define the CFR as the number of observed deaths one-week ahead divided by this week’s observed cases. The IFR is defined as the number of estimated deaths one-week ahead divided by this week’s estimated cases. Before turning to the figure, we note that over our entire sample, the CFR is 2.6%, while the IFR ranges from 0.9% to 2.1%, with the 0.9% coming from the time-varying decay model which follows from the fact that this model produces the highest estimated caseload.

³⁹To incorporate such a restriction into the estimation would require perhaps directly modeling the cumulative infection rate and combining a stochastic frontier model with a fractional logit/probit setup. This is beyond the scope of the current paper. Alternatively, one could predict cases in these instances using a confidence bound (Simar & Wilson 2010).

The fact that our estimates of the IFR are below the CFR results from our estimate of more missing cases than deaths.⁴⁰ Regardless, one important finding from this is that the COVID-19 virus is less lethal than what is commonly reported in the news media (based on the CFR).

Turning to the figure, we see that the CFR and IFRs peak very early in the pandemic for the US, and for most of the world, outside of later spikes in Sub-Saharan Africa and East Asia and the Pacific. Since the late summer, there is little difference between the CFR and the estimated IFRs for Europe and East Asia, North America, and Middle East and North Africa. The steady decline of the CFR/IFRs is likely due to increased experience handling the virus, improvements in therapeutics, and heightened public awareness. Finally, it is noteworthy that there is apparent convergence between the CFR and the IFRs as we enter the later stages of the pandemic. The one exception is the Latin American and Caribbean region; the CFR and IFRs have yet to converge. Thus, for this region, the lethality of the disease appears to be much lower in magnitude than suggested by the CFR even in Fall 2020.⁴¹

4.3 Country- & Time-Specific Infection Rates, Fatality Rates, and Recovery Rates

We use the model estimates in one final manner. As discussed in Section 3.1, the reproduction number, R_{0it} , is equal to $\beta_{it}/(\gamma_{1it} + \gamma_{2it})$, where β_{it} is the infection rate, γ_{1it} is the recovery rate, and γ_{2it} is the fatality rate. Using equations (11) and (16) and assuming that each has a lognormal distribution, β_{it} and γ_{2it} are consistently estimated by

$$\hat{\beta}_{it} = \exp\left(X\hat{\beta} + \frac{1}{2}\sigma_{v\beta}^2\right) \quad (22)$$

$$\hat{\gamma}_{2it} = \exp\left(X\hat{\gamma} + \frac{1}{2}\sigma_{v\gamma}^2\right), \quad (23)$$

where $\sigma_{v\beta}^2$ and $\sigma_{v\gamma}^2$ are the variances of v^β and v^γ , respectively.⁴²

These are plotted in Figures A3 and A4 for select countries. For the US, the infection rate has increased at the start of the pandemic, slowed and perhaps even dipped during the summer, and recently has begun to increase again. Estimates of the infection rate at the end of our sample range from roughly 0.7% to 1.3%. Other countries shown also have seen an increase in the infection rate this fall with the exception of South Korea. The fatality rates, on the other hand, have declined since the summer in the majority of the countries shown; Brazil, and to a lesser extent Italy, are the exceptions.

As we do not have data on recoveries from COVID-19, we cannot directly estimate γ_{1it} and, hence, cannot estimate R_{0it} . However, to provide some information on the recovery rate we use available estimates for R_{0it} , combined with our estimates of β_{it} and γ_{2it} , to obtain estimates of γ_{1it} .⁴³ Specifically, estimates of γ_{1it} are given by

$$\hat{\gamma}_{1it} = \frac{\beta_{it} - \gamma_{2it}R_{0it}}{R_{0it}}. \quad (24)$$

⁴⁰Manski & Molinari (2020) reach a similar conclusion; however, they assume that deaths are reported correctly.

⁴¹We investigated whether the lack of convergence in the CFR and IFRs is driven by Brazil. Omitting Brazil from the analysis does not change this finding; if anything, the divergence at the end of the sample period is even greater.

⁴²In practice, $\sigma_{v\beta}^2$ and $\sigma_{v\gamma}^2$ are not identified. Instead, we use σ_{vY}^2 and σ_{vD}^2 . See equations (12) and (17).

⁴³Estimates are provided at <http://metrics.covid19-analysis.org/>. They are obtained using the EpiEstim method implemented using the EpiEstim R package.

As the estimates of R_{0it} do not account for under-reporting, the results should be viewed cautiously.

These are plotted in Figures A5. For the US, the recovery rate increased from the spring to the summer and has remained relatively constant since. Estimates of the infection rate at the end of our sample range from roughly 0.6% to 1.1%. The other countries examined also show similar rises in the recovery rate entering Fall 2020. South Korea is the lone exception. However, this is consistent with the low infection rate in South Korea (see Figure A3) that also shows no signs of increasing entering Fall 2020.

5 Conclusion

Not since the Spanish Flu of 1918-1919 has the world faced a public health crisis of the magnitude of COVID-19. Meeting this challenge is made more difficult due to the lack of complete information. Understanding the science behind the SARS-CoV-2 virus and the COVID-19 disease and devising optimal policy responses requires accurate data. Unfortunately, missing data are rampant. The reasons for this are numerous and diverse, ranging from the apparently high rate of asymptomatic cases to inadequate surveillance systems to political corruption.

In this paper, we devise a method to overcome this missing data problem. A ‘structural’ model based on the SIR framework extended to allow for measurement error yields estimating equations for cases and deaths that conveniently resembles the classic stochastic frontier model. This connection has not been made to our knowledge and represents a tractable approach to incorporate missing data into the standard SIR model.

Admittedly, the stochastic frontier model relies on strong distributional assumptions. While these assumptions change the magnitude of our conclusions, they do not change our fundamental conclusions. Further, as shown in Badunenko et al. (2012), the setting we are operating in is perhaps the most robust to discrepancies in the distributional assumptions: a large degree of under-reporting relative to the stochastic noise present overall. Moreover, the assumptions of the stochastic frontier model are orthogonal to the strong assumptions made in other studies seeking to overcome missing data to assess the pandemic. Thus, we view our approach as adding to the totality of our knowledge. Seen in this light, we find it reassuring that our range of predictions align with the limited existing research seeking to understand both the extent of the COVID-19 pandemic, as well as the ability of NPIs and testing to limit the scope of it.

Specifically, our approach yields a multiplication factor for the true number of cases between two and nine; a multiplication factor of the true number of deaths between 1.6 to 3.0. Our approach yields an infectious fatality rate ranging from 0.9% to 2.1%, in contrast to a case fatality rate of 2.6%. The fact that our estimates of the infectious fatality rate are below the case fatality rate results from our estimate of more missing cases than deaths.

Our analysis here suggests a number of avenues for future research that should prove fruitful in modeling pandemics with missing data. First, as noted, our estimated cumulative infection rates exceed 100% for some countries in our sample in some specifications. Adjusting the functional form to constrain the number of infections by the total population of the country (or some fraction thereof), while not immediately obvious, would be valuable. While this might entail placing bounds on the degree of under-counting, making the model more similar to existing approaches and less similar to a standard stochastic frontier setting, this could potentially be done using the doubled-bounded efficiency estimator in Almanidis et al. (2014) or a Tobit-type estimator which truncates the degree of under-counting based on the population

of the country. Or, as mentioned previously, directly modeling the cumulative infection rate, rather than new cases, and constraining the rate to be in the unit interval as in fractional logit/probit models.

Second, our estimation procedure has focused on cases and deaths separately. Joint estimation might exploit information in cases to improve estimation of actual deaths. However, doing so risks mis-specification in one equation leading to bias in the other. Finally, future research might consider modeling under-reporting of cases and deaths as a deterministic function of a set of observable covariates, thereby reducing reliance on distributional assumptions. If the covariates that determine the quality of the data – such as testing and reporting protocols, inclusivity of surveillance systems, rigor of contact tracing, dissemination of information, etc. – are measurable, such a model may be informative.

We conclude by re-iterating our message at the outset: no model addressing missing data is beyond reproach. While the stochastic frontier SIR model we propose requires assumptions on the nature of under-reporting of cases and deaths, so too do other methods that have recently received critical attention. Rather than relying on any single model, and hence set of assumptions, scientists and policymakers ought to aggregate information across a wide range of methodologies. Stochastic frontier modeling should be part of this set.

References

- Aigner, D. J., Lovell, C. A. K. & Schmidt, P. (1977), ‘Formulation and estimation of stochastic frontier production functions’, *Journal of Econometrics* **6**(1), 21–37.
- Almanidis, P., Qian, J. & Sickles, R. C. (2014), Stochastic frontier models with bounded inefficiency, in R. C. Sickles & W. C. Horrace, eds, ‘Festschrift in Honor of Peter Schmidt Econometric Methods and Applications’, Springer: New York, pp. 47–82.
- Arroyo-Marioli, F., Bullano, F., Kučinskas, S. & Rondón-Moreno, C. (2020), ‘Tracking R of COVID-19: A new real-time estimation using the kalman filter’, *medRxiv* .
URL: <https://www.medrxiv.org/content/early/2020/04/29/2020.04.15.20066431>
- Askatas, N., Tatsiramos, K. & Verheyden, B. (2020), Lockdown strategies, mobility patterns and COVID-19. IZA DP NO. 13293.
- Atkeson, A. (2020), How deadly is COVID-19? understanding the difficulties with estimation of its fatality rate. NBER Working Paper No. 26965.
- Avery, C., Bossert, W., Clark, A., Ellison, G. & Fisher Ellison, S. (2020), ‘An economist’s guide to epidemiology models of infectious disease’, *Journal of Economic Perspectives* **34**, 79–104.
- Backhaus, A. (2020), ‘Common pitfalls in the interpretation of COVID-19 data and statistics’, *Intereconomics* **55**, 162–166.
- Badunenko, O., Henderson, D. J. & Kumbhakar, S. C. (2012), ‘When, where and how to perform efficiency analysis’, *Journal of the Royal Statistical Society, Series A* **175**(4), 863–892.
- Bellemare, M. F. & Wichman, C. J. (2020), ‘Elasticities and the inverse hyperbolic sine transformation’, *Oxford Bulletin of Economics and Statistics* **82**, 50–61.
- Chernozhukov, V., Kasahara, H. & Schrimpf, P. (2020), ‘Causal impact of masks, policies, behavior on early COVID-19 pandemic in the U.S.’, *Journal of Econometrics* . Forthcoming.
- Chudik, A., Pesaran, M. H. & Rebucci, A. (2020), Voluntary and mandatory social distancing: Evidence on Covid-19 exposure rates from Chinese provinces and select countries. NBER Working paper 27039.
- Dang, H.-A. & Trinh, T.-A. (2020), The beneficial impacts of covid-19 lockdowns on air pollution: Evidence from vietnam. IZA Discussion Paper No. 13651.
- Depalo, D. (2021), ‘True COVID-19 mortality rates from administrative data’, *Journal of Population Economics* **34**, 253–274.
- Fetzer, T. & Graeber, T. (2020), Does contact tracing work? quasi-experimental evidence from an excel error in england. CAGE Working Paper No. 521.
- Flaxman, S., Mishra, S., Gandy, A., Unwin, H. J. T., Mellan, T. A., Coupland, H., Whittaker, C., Zhu, H., Berah, T., Eaton, J. W., Monod, M., Perez-Guzman, P. N., Schmit, N., Cilloni, L., Ainslie, K.

- E. C., Baguelin, M., Boonyasiri, A., Boyd, O., Cattarino, L., Cooper, L. V., Cucunubá, Z., Cuomo-Dannenburg, G., Dighe, A., Djaafara, B., Dorigatti, I., van Elsland, S. L., FitzJohn, R. G., Gaythorpe, K. A. M., Geidelberg, L., Grassly, N. C., Green, W. D., Hallett, T., Hamlet, A., Hinsley, W., Jeffrey, B., Knock, E., Laydon, D. J., Nedjati-Gilani, G., Nouvellet, P., Parag, K. V., Siveroni, I., Thompson, H. A., Verity, R., Volz, E., Walters, C. E., Wang, H., Wang, Y., Watson, O. J., Winskill, P., Xi, X., Walker, P. G. T., Ghani, A. C., Donnelly, C. A., Riley, S. M., Vollmer, M. A. C., Ferguson, N. M., Okell, L. C., Bhatt, S. & Team, I. C. C.-. R. (2020), ‘Estimating the effects of non-pharmaceutical interventions on COVID-19 in Europe’, *Nature* . Forthcoming.
- Gibbons, C. L., Mangen, M.-J. J., Plass, D., Havelaar, A. H., Brooke, R. J., Kramarz, P., Peterson, K. L., Stuurman, A. L., Cassini, A., Fèvre, E. M. & Kretzschmar, M. E. E. (2014), ‘Measuring underreporting and under-ascertainment in infectious disease datasets: a comparison of methods’, *BMC Public Health* **14**(1), 147–164.
- Goolsbee, A. & Syverson, C. (2020), Fear, lockdown, and diversion: Comparing drivers of pandemic economic decline 2020. NBER Working Paper No. 27432.
- Hale, T., Webster, S., Petherick, A., Phillips, T. & Kira, B. (2020), Oxford COVID-19 Government Response Tracker. Blavatnik School of Government. Available: www.bsg.ox.ac.uk/covidtracker.
- Hortaçsu, A., Liu, J. & Schieg, T. (2020), ‘Estimating the fraction of unreported infections in epidemics with a known epicenter: An application to COVID-19’, *Journal of Econometrics* . Forthcoming.
- Jondrow, J., Lovell, C. A. K., Materov, I. S. & Schmidt, P. (1982), ‘On the estimation of technical efficiency in the stochastic frontier production function model’, *Journal of Econometrics* **19**(2/3), 233–238.
- Kermack, W. O. & McKendrick, A. G. (1927), ‘A contribution to the mathematical theory of epidemics’, *Proceedings of the Royal Society A* **115**, 700–721.
- Korolev, I. (2020), ‘Identification and estimation of the SEIRD epidemic model for COVID-19’, *Journal of Econometrics* . Forthcoming.
- Li, R., Pei, S., Chen, B., Song, Y., Zhang, T., Yang, W. & Shaman, J. (2020), ‘Substantial undocumented infection facilitates the rapid dissemination of novel coronavirus (SARS-CoV-2)’, *Science* **368**(6490), 489–493.
- Li, S. & Linton, O. (2020), ‘When will the COVID-19 pandemic peak’, *Journal of Econometrics* . Forthcoming.
- Manski, C. F. & Molinari, F. (2020), ‘Estimating the COVID-19 infection rate: Anatomy of an inference problem’, *Journal of Econometrics* . Forthcoming.
- Meeusen, W. & van den Broeck, J. (1977), ‘Efficiency estimation from Cobb-Douglas production functions with composed error’, *International Economic Review* **18**(2), 435–444.
- Millimet, D. L. & Parmeter, C. F. (2020), ‘Accounting for skewed or one-sided measurement error in the dependent variable’, *Political Analysis* . Forthcoming.

- Murray, E. J. (2020), ‘Epidemiology’s time of need: COVID-19 calls for epidemic-related economics’, *Journal of Economic Perspectives* **34**, 105–120.
- Oguzoglu, U. (2020), Covid-19 lockdowns and decline in traffic related deaths and injuries. IZA Discussion Paper No. 13278.
- Papadopoulos, A. & Parmeter, C. F. (2020), Moment diagnostics and quasi-maximum likelihood estimation for the stochastic frontier model. Working Paper, University of Miami.
- Parmeter, C. F. & Kumbhakar, S. C. (2014), ‘Efficiency Analysis: A Primer on Recent Advances’, *Foundations and Trends in Econometrics* **7**(3-4), 191–385.
- Pitt, M. M. & Lee, L.-F. (1981), ‘The measurement and sources of technical inefficiency in the Indonesian weaving industry’, *Journal of Development Economics* **9**(1), 43–64.
- Reed, C., Angulo, F. J., Swerdlow, D. L., Lipsitch, M., Meltzer, M. I., Jernigan, D. & Finelli, L. (2009), ‘Estimates of the prevalence of pandemic (H1N1) 2009, United States, April–July 2009’, *Emerging Infectious Diseases* **15**(12), 2004–2007.
- Reese, H., Iuliano, A. D., Patel, N. N., Garg, S., Kim, L., Silk, B. J., Hall, A. J., Fry, A. & Reed, C. (2020), ‘Estimated incidence of COVID-19 illness and hospitalization — united states, february–september, 2020’, *Clinical Infectious Diseases* . Forthcoming.
- Sá, F. (2020), Socioeconomic determinants of COVID-19 infections and mortality: Evidence from England and Wales. IZA Policy Paper No. 159.
- Simar, L. & Wilson, P. W. (2010), ‘Inferences from cross-sectional, stochastic frontier models’, *Econometric Reviews* **29**(1), 62–98.
- Stock, J. H. (2020), Random testing is urgently needed. Manuscript, available at: <http://www.igmchicago.org/covid-19/random-testing-is-urgently-needed/>.
- Sutton, D., Fuchs, K., D’Alton, M. & Goffman, D. (2020), ‘Universal screening for SARS-CoV-2 in women admitted for delivery’, *New England Journal of Medicine* **382**(22), 2163–2164.
- Teixeira da Silva, J. & Tsigaris, P. (2020), ‘Policy determinants of COVID-19 pandemic induced fatality rate across nations’, *Public Health* **187**, 140–142.
- Weinberger, D., Cohen, T., Crawford, F., Mostashari, F., Olson, D., Pitzer, V. E., Reich, N. G., Russi, M., Simonsen, L., Watkins, A. & Viboud, C. (2020), ‘Estimating the early death toll of COVID-19 in the United States’, *medRxiv* .
URL: <https://www.medrxiv.org/content/early/2020/04/29/2020.04.15.20066431>

Tables & Figures

Table 1: Countries included in sample.

Afghanistan	Ecuador	Japan	Romania
Algeria	Egypt	Kuwait	Russia
Australia	Estonia	Lebanon	San Marino
Austria	Finland	Lithuania	Singapore
Azerbaijan	France	Luxembourg	South Korea
Bahrain	Georgia	Malaysia	Spain
Belarus	Germany	Mexico	Sri Lanka
Belgium	Greece	Nepal	Sweden
Brazil	Iceland	Netherlands	Switzerland
Cambodia	India	New Zealand	Taiwan
Canada	Indonesia	Nigeria	Thailand
China	Iran	Norway	United Arab Emirates
Croatia	Iraq	Oman	United Kingdom
Czech Republic	Ireland	Pakistan	United States
Denmark	Israel	Philippines	Vietnam
Dominican Republic	Italy	Qatar	

Table 2: Stochastic frontier results assuming independence

	Half Normal		Exponential	
	Cases (1)	Deaths (2)	Cases (3)	Deaths (4)
Lagged Containment Index	0.020 (0.016)	0.006 (0.015)	0.017 (0.016)	0.006 (0.016)
(Lagged Containment Index) ²	-0.000* (0.000)	-0.000 (0.000)	-0.000 (0.000)	-0.000 (0.000)
(Lagged Containment Index) × (Linear Time Trend)	0.001 (0.000)	0.001 (0.000)	0.000 (0.000)	0.001 (0.000)
New Tests _{t-1}	-0.185 (0.128)	0.523** (0.225)	-0.193 (0.139)	0.537** (0.215)
(New Tests _{t-1}) ²	0.045*** (0.010)	-0.035** (0.016)	0.045*** (0.011)	-0.035** (0.015)
(New Tests _{t-1}) × (Linear Time Trend)	-0.008*** (0.002)	-0.004* (0.002)	-0.007*** (0.002)	-0.004* (0.002)
(New Tests _{t-1})×I(Test Units = People)	-0.535*** (0.194)	-1.204*** (0.270)	-0.523** (0.209)	-1.222*** (0.262)
(New Tests _{t-1} ×I(Test Units = People)) ²	0.033* (0.017)	0.096*** (0.023)	0.033* (0.018)	0.098*** (0.021)
(New Tests _{t-1} ×I(Test Units = People)) × (Linear Time Trend)	0.003 (0.003)	0.003 (0.003)	0.002 (0.003)	0.002 (0.003)
(New Tests _{t-1})×I(Test Units = Samples)	0.101 (0.193)	-1.072*** (0.282)	0.080 (0.208)	-1.088*** (0.270)
(New Tests _{t-1} ×I(Test Units = Samples)) ²	-0.009 (0.020)	0.104*** (0.022)	-0.005 (0.020)	0.105*** (0.021)
(New Tests _{t-1} ×I(Test Units = Samples)) × (Linear Time Trend)	0.003 (0.003)	0.001 (0.004)	0.002 (0.003)	0.001 (0.004)
(New Tests _{t-1})×I(Test Units = Tests)	-0.188 (0.164)	-1.048*** (0.288)	-0.226 (0.172)	-1.070*** (0.266)
(New Tests _{t-1} ×I(Test Units = Tests)) ²	-0.005 (0.012)	0.075*** (0.021)	-0.003 (0.013)	0.076*** (0.020)
(New Tests _{t-1} ×I(Test Units = Tests)) × (Linear Time Trend)	0.003* (0.002)	0.004* (0.002)	0.003** (0.002)	0.004* (0.002)
N	2195	1712	2195	1712
Marginal Effect: Lagged Containment Index	-0.001 (0.006)	-0.009 (0.006)	-0.001 (0.006)	-0.009 (0.007)
Observed (Cumulative)	p = 0.934 37,663,440	p = 0.156 980,123	p = 0.909 37,663,440	p = 0.162 980,123
Predicted (Cumulative)	109,767,009	2,108,317	73,746,440	1,534,761

Standard errors in parentheses. Half normal model assumes $u_{it} \sim N^+(0, \sigma_u^2)$. Exponential model assumes $u_{it} \sim \exp(\lambda)$. $I(\cdot)$ is the indicator function, equal to one if the argument is true and zero otherwise. Lagged containment index is the average of the third and fourth lags in the models for cases; fifth and sixth lags for deaths. Number of tests is transformed using the inverse hyperbolic sine. Other covariates included in all models: log population, population density, median age, percent of population aged 65+, percent of population with diabetes, log per capita Gross Domestic Product, corruption index, the quadratic of each of the preceding variables, region fixed effects, and region-specific time trends. * $p < .10$, ** $p < .05$, *** $p < .01$.

Table 3: Stochastic frontier results allowing for dependence

	Time-Varying		Time Invariant	
	Measurement Error	Measurement Error	Measurement Error	Measurement Error
	Cases	Deaths	Cases	Deaths
	(1)	(2)	(3)	(4)
Lagged Containment Index	0.031*** (0.007)	-0.008 (0.007)	0.028*** (0.007)	-0.004 (0.007)
(Lagged Containment Index) ²	-0.000 (0.000)	0.000 (0.000)	-0.000* (0.000)	0.000 (0.000)
(Lagged Containment Index) × (Linear Time Trend)	-0.001*** (0.000)	-0.001** (0.000)	-0.001*** (0.000)	-0.000* (0.000)
(New Tests _{t-1})	0.031 (0.243)	0.334 (0.378)	-0.076 (0.244)	0.223 (0.380)
(New Tests _{t-1}) ²	0.034 (0.024)	-0.017 (0.034)	0.036 (0.025)	-0.015 (0.035)
(New Tests _{t-1}) × (Linear Time Trend)	-0.010*** (0.003)	-0.005 (0.004)	-0.007** (0.003)	-0.002 (0.004)
(New Tests _{t-1}) × I(Test Units = People)	-0.313 (0.269)	-0.631 (0.401)	-0.225 (0.270)	-0.728* (0.406)
(New Tests _{t-1}) × I(Test Units = People) ²	0.014 (0.026)	0.059* (0.036)	0.018 (0.027)	0.072* (0.037)
(New Tests _{t-1}) × I(Test Units = People) × (Linear Time Trend)	0.006* (0.003)	0.005 (0.004)	0.001 (0.003)	0.000 (0.004)
(New Tests _{t-1}) × I(Test Units = Samples)	-0.081 (0.257)	-0.856** (0.392)	-0.135 (0.256)	-0.755* (0.392)
(New Tests _{t-1}) × I(Test Units = Samples) ²	-0.006 (0.025)	0.077** (0.035)	0.005 (0.026)	0.078** (0.036)
(New Tests _{t-1}) × I(Test Units = Samples) × (Linear Time Trend)	0.004 (0.003)	0.003 (0.004)	0.002 (0.003)	-0.000 (0.004)
(New Tests _{t-1}) × I(Test Units = Tests)	-0.433* (0.249)	-1.024*** (0.385)	-0.299 (0.251)	-0.864** (0.386)
(New Tests _{t-1}) × I(Test Units = Tests) ²	0.017 (0.025)	0.073** (0.034)	0.014 (0.025)	0.067* (0.035)
(New Tests _{t-1}) × I(Test Units = Tests) × (Linear Time Trend)	0.004 (0.003)	0.005 (0.004)	0.001 (0.003)	0.001 (0.004)
N	2195	1712	2195	1712
Marginal Effect: Lagged Containment Index	-0.015*** (0.003)	-0.014*** (0.003)	-0.007*** (0.003)	-0.010*** (0.003)
Observed (Cumulative)	p = 0.000 37,663,440	p = 0.000 980,123	p = 0.006 37,663,440	p = 0.001 980,123
Predicted (Cumulative)	337,360,283	2,954,841	130,411,499	1,849,022

Standard errors in parentheses. Time invariant model assumes $u_i \sim N^+(0, \sigma_u^2)$. The time-varying model assumes $u_{it} = \exp\{-\eta(t - T_i)\}u_i$, $u_i \sim N^+(0, \sigma_u^2)$. $I(\cdot)$ is the indicator function, equal to one if the argument is true and zero otherwise. Lagged containment index is the average of the third and fourth lags in the models for cases; fifth and sixth lags for deaths. Number of tests is transformed using the inverse hyperbolic sine. Other covariates included in all models: log population, population density, median age, percent of population aged 65+, percent of population with diabetes, log per capita Gross Domestic Product, corruption index, the quadratic of each of the preceding variables, region fixed effects, and region-specific time trends. * p < .10, ** p < .05, *** p < .01.

Table 4: Country-specific multiplication factors.

Country	Cases				Deaths			
	Half-Normal	Exponential	Time-Varying	Time Invariant	Half-Normal	Exponential	Time-Varying	Time Invariant
	(1)	(2)	(3)	(4)	(5)	(6)	(7)	(8)
Afghanistan	2.846	1.731	106.986	1.749	2.214	1.583	2.856	1.664
Algeria	5.188	2.498	8.397	3.039	3.409	1.938	4.208	7.599
Australia	2.029	1.584	1.704	1.360	1.579	1.351	1.218	1.218
Austria	2.642	1.787	6.025	4.220	2.128	1.549	5.061	2.252
Azerbaijan	2.843	1.914	1.550	1.414	3.376	1.941	2.988	6.371
Bahrain	3.336	2.163	1.439	2.091	2.492	1.687	1.897	1.616
Belarus	2.465	1.785	1.963	1.514	2.913	1.800	4.504	4.285
Belgium	1.944	1.585	1.460	2.169	1.682	1.397	2.967	1.310
Brazil	2.070	1.640	2.116	1.259	2.072	1.545	2.175	1.286
Cambodia	7.006	3.293	71.152	7.550				
Canada	4.247	2.311	6.843	1.414	2.292	1.608	1.600	2.114
China	3.001	1.817	6.473	7.332	1.589	1.357	7.377	15.410
Croatia	2.228	1.680	28.549	6.668	1.943	1.487	1.472	3.060
Czech Republic	2.295	1.713	1.807	5.685	1.993	1.489	3.733	4.942
Denmark	4.496	2.371	9.436	5.131	2.296	1.605	11.659	3.936
Dominican Republic	2.865	1.958	1.451	1.374	2.754	1.761	2.408	1.538
Ecuador	4.841	2.470	99.026	12.068	2.334	1.615	11.456	3.814
Egypt	2.968	1.735	12.432	1.273	1.866	1.464	3.589	1.249
Estonia	3.106	1.937	10.947	2.549	2.337	1.687	4.930	2.964
Finland	3.441	2.081	4.544	2.939	1.908	1.484	7.726	2.549
France	3.492	2.143	7.926	9.219	2.005	1.512	6.777	3.563
Georgia	2.090	1.590	3.451	5.880	1.618	1.376	1.404	1.343
Germany	4.235	2.221	12.718	6.969	2.049	1.530	5.730	1.981
Greece	2.760	1.867	1.467	1.783	2.120	1.545	1.249	1.343
Iceland	2.857	1.867	7.098	2.997				
India	2.854	2.008	1.569	1.826	2.669	1.739	1.744	1.592
Indonesia	1.787	1.555	1.215	1.166	1.709	1.411	1.176	1.149
Iran	2.424	1.822	4.025	1.511	1.777	1.440	1.218	1.219
Iraq	2.974	2.081	4.454	1.568	2.000	1.518	1.283	1.299
Ireland	2.810	1.864	3.188	2.047	1.774	1.430	2.604	1.468
Israel	4.304	2.471	1.471	7.191	3.175	1.880	12.046	10.611
Italy	4.340	2.342	21.337	11.324	1.900	1.477	1.909	1.620
Japan	2.387	1.753	1.478	1.411	2.491	1.666	1.854	1.511
Kuwait	2.554	1.843	1.719	1.263	2.094	1.548	2.565	1.232
Lebanon	1.807	1.538	1.710	1.300	2.351	1.640	2.338	3.206
Lithuania	1.982	1.564	1.521	1.249	1.952	1.495	1.646	1.325
Luxembourg	2.260	1.672	1.789	1.270	1.804	1.461	2.460	1.313
Malaysia	2.525	1.714	12.951	2.279	2.221	1.588	10.283	4.926
Mexico	8.117	3.164	179.189	16.781	2.269	1.612	2.849	1.776
Nepal	1.859	1.573	1.482	1.295	2.163	1.572	2.703	1.429
Netherlands	1.981	1.587	1.657	1.221	1.773	1.431	1.288	1.177
New Zealand	2.295	1.626	2.341	1.603				
Nigeria	5.353	2.629	49.543	3.531	2.876	1.794	76.622	4.349
Norway	10.164	3.848	176.037	19.166	3.008	1.843	22.919	17.060
Oman	3.164	1.987	3.424	3.009	2.172	1.577	1.649	1.755
Pakistan	4.583	2.332	31.946	4.445	2.244	1.592	2.030	2.275
Philippines	2.408	1.822	1.272	1.685	2.365	1.636	5.529	4.348
Qatar	4.250	2.266	8.001	5.039	2.840	1.779	32.713	6.550
Romania	2.973	1.958	1.250	3.263	2.088	1.540	1.072	1.295
Russia	3.186	2.063	5.842	4.088	2.945	1.818	3.207	5.706
Singapore	2.760	1.852	23.178	1.552				
South Korea	2.836	1.807	8.942	4.411	2.043	1.526	1.473	2.037
Spain	2.136	1.662	1.100	1.148	1.709	1.412	1.215	1.310
Sri Lanka	3.973	2.127	21.326	2.180				
Sweden	2.427	1.790	2.203	1.220	1.928	1.490	4.071	1.679
Switzerland	1.869	1.525	4.780	2.375	1.771	1.429	5.032	1.470
Thailand	4.043	2.141	8.783	5.232	3.698	2.160	5.896	11.612
United Arab Emirates	5.320	2.589	55.226	8.187	3.263	1.893	307.806	6.642
United Kingdom	3.959	2.264	14.934	11.819	1.795	1.434	10.593	2.713
United States	2.602	1.924	1.483	2.721	2.096	1.552	1.387	1.372
Vietnam	5.275	2.823	4.220	11.792	2.494	1.754	38.478	7.990

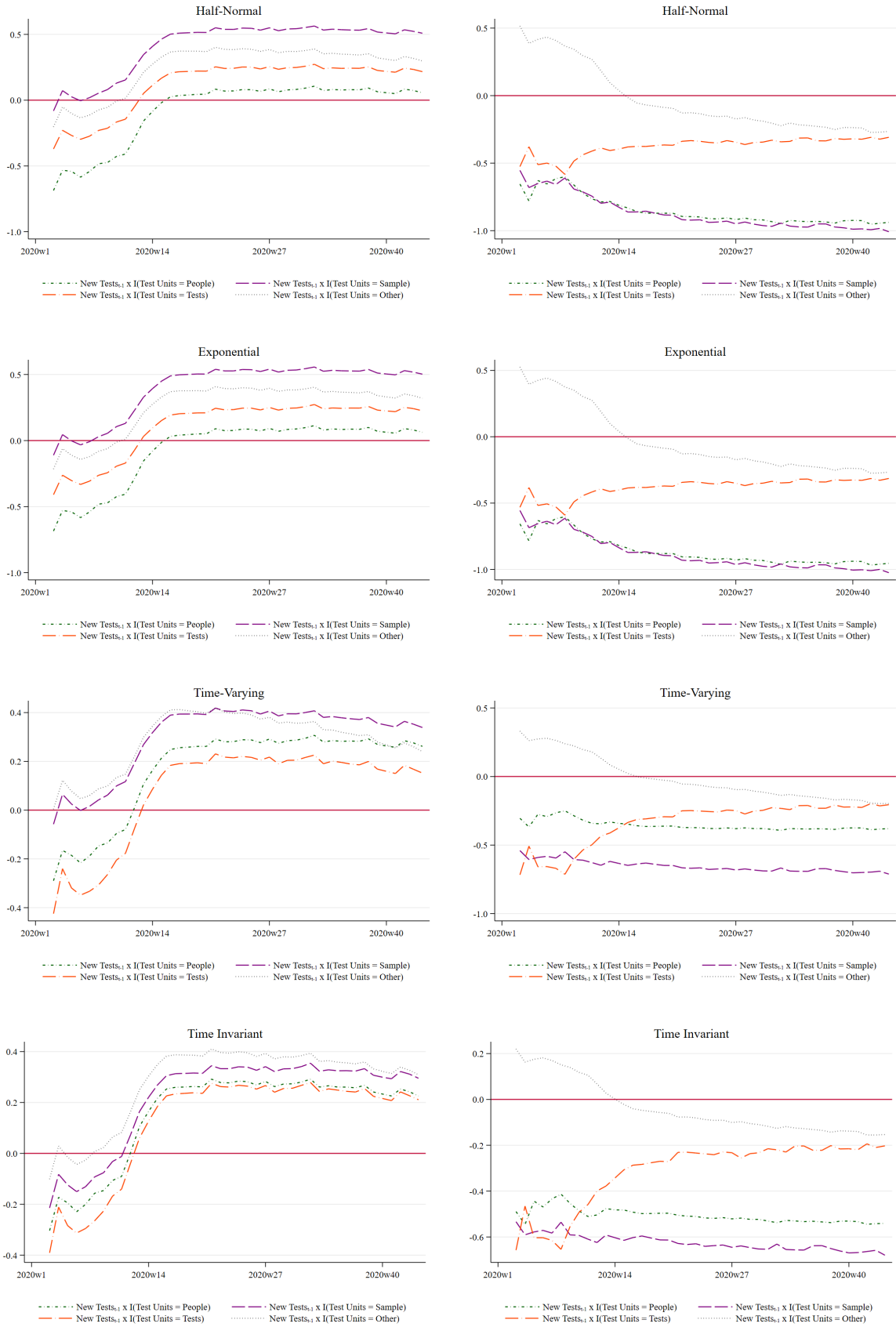
Multiplication factor is defined as the total number of estimated cases or deaths divided by the total number of reported cases or deaths.

Table 5: Observed and predicted country-specific cumulative infection rates.

Country	Observed	Predicted			
	(1)	Half-Normal (2)	Exponential (3)	Time Invariant (4)	Time-Varying (5)
Afghanistan	0.107	0.305	0.186	0.187	11.467
Algeria	0.134	0.693	0.334	0.406	1.122
Australia	0.108	0.220	0.171	0.147	0.184
Austria	1.269	3.352	2.267	5.355	7.645
Azerbaijan	0.563	1.599	1.076	0.795	0.872
Bahrain	4.827	16.104	10.441	10.095	6.946
Belarus	1.063	2.619	1.896	1.609	2.085
Belgium	3.846	7.476	6.098	8.342	5.615
Brazil	2.613	5.410	4.285	3.291	5.529
Cambodia	0.002	0.012	0.006	0.013	0.123
Canada	0.637	2.704	1.471	0.900	4.356
China	0.005	0.015	0.009	0.036	0.032
Croatia	1.283	2.858	2.156	8.553	36.621
Czech Republic	3.277	7.520	5.614	18.629	5.921
Denmark	0.833	3.744	1.975	4.273	7.859
Dominican Republic	1.176	3.370	2.303	1.616	1.707
Ecuador	1.100	5.325	2.717	13.275	108.925
Egypt	0.105	0.313	0.183	0.134	1.311
Estonia	0.380	1.181	0.737	0.969	4.163
Finland	0.296	1.018	0.616	0.870	1.345
France	2.249	7.852	4.818	20.733	17.825
Georgia	1.067	2.230	1.697	6.275	3.684
Germany	0.669	2.833	1.485	4.661	8.506
Greece	0.404	1.114	0.754	0.720	0.592
Iceland	1.445	4.128	2.698	4.331	10.257
India	0.599	1.710	1.203	1.094	0.940
Indonesia	0.152	0.271	0.236	0.177	0.184
Iran	0.749	1.814	1.364	1.132	3.014
Iraq	1.190	3.540	2.477	1.866	5.301
Ireland	1.271	3.571	2.369	2.601	4.051
Israel	3.651	15.712	9.022	26.250	5.372
Italy	1.210	5.253	2.835	13.708	25.829
Japan	0.081	0.193	0.142	0.114	0.120
Kuwait	2.981	7.612	5.494	3.765	5.124
Lebanon	1.226	2.216	1.886	1.594	2.097
Lithuania	0.616	1.221	0.963	0.769	0.937
Luxembourg	3.493	7.895	5.841	4.435	6.250
Malaysia	0.103	0.260	0.176	0.235	1.334
Mexico	0.724	5.875	2.290	12.145	129.688
Nepal	0.606	1.126	0.953	0.784	0.898
Netherlands	2.146	4.250	3.405	2.620	3.556
New Zealand	0.033	0.076	0.054	0.053	0.078
Nigeria	0.031	0.164	0.080	0.108	1.515
Norway	0.381	3.869	1.465	7.295	67.002
Oman	2.274	7.197	4.520	6.843	7.787
Pakistan	0.152	0.698	0.355	0.677	4.863
Philippines	0.352	0.847	0.641	0.593	0.447
Qatar	4.613	19.608	10.455	23.246	36.910
Romania	1.303	3.875	2.552	4.252	1.628
Russia	1.134	3.613	2.339	4.636	6.625
Singapore	0.991	2.737	1.836	1.539	22.980
South Korea	0.052	0.148	0.094	0.231	0.467
Spain	2.658	5.679	4.417	3.051	2.924
Sri Lanka	0.053	0.210	0.113	0.115	1.129
Sweden	1.231	2.988	2.204	1.503	2.712
Switzerland	2.029	3.791	3.094	4.818	9.697
Thailand	0.005	0.022	0.012	0.028	0.048
United Arab Emirates	1.366	7.268	3.538	11.185	75.452
United Kingdom	1.552	6.146	3.515	18.347	23.184
United States	2.807	7.305	5.400	7.639	4.163
Vietnam	0.001	0.006	0.003	0.014	0.005

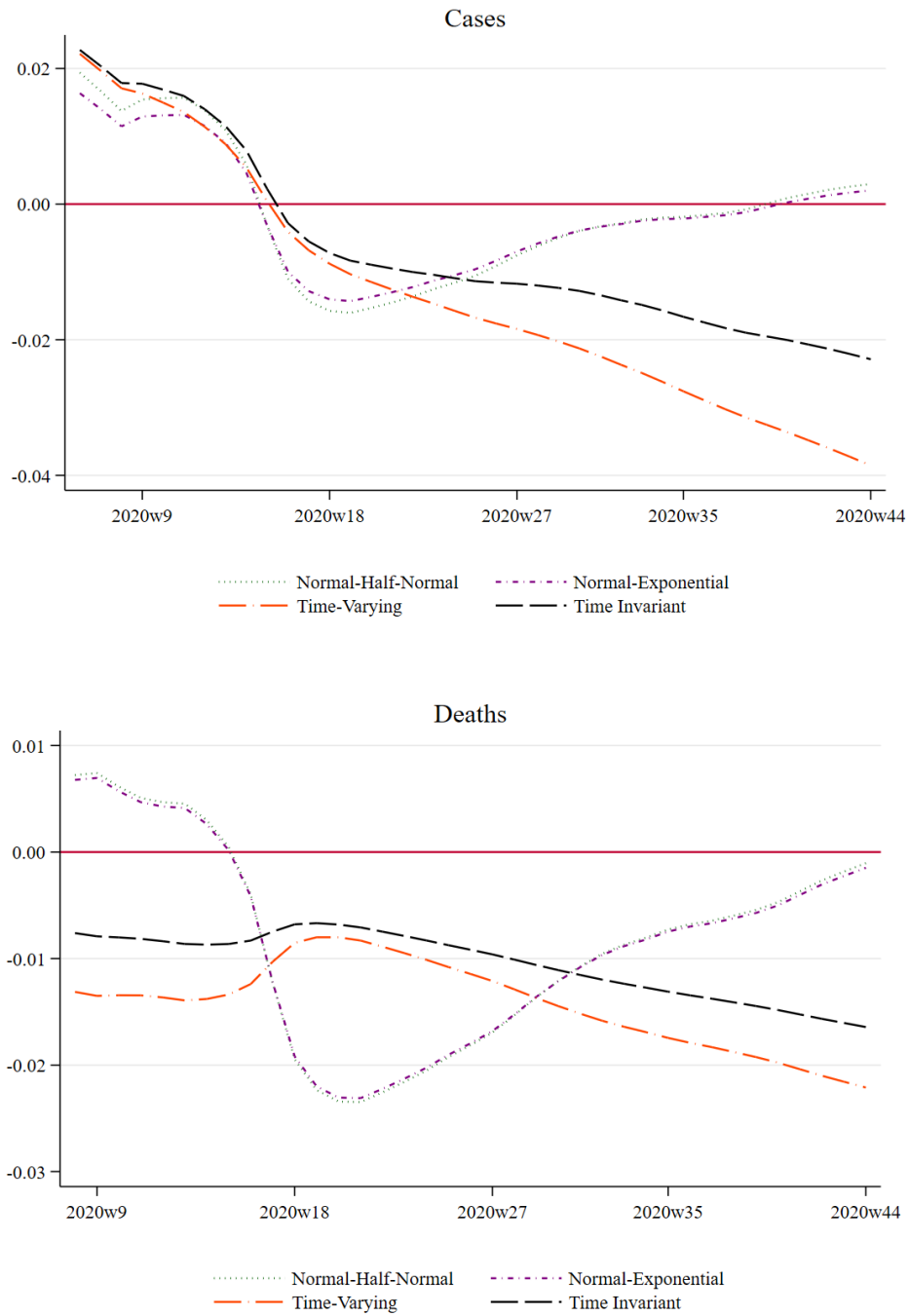
Infection rate is defined as the total number of cases – observed in column (1) or predicted in columns (2)-(5) – divided by population (multiplied by 100).

Figure 1: Marginal effects of testing on cases and deaths.



Marginal effects on cases are in the left column. Marginal effects on deaths are in the right column.

Figure 2: Marginal effects of non-pharmaceutical interventions on cases and deaths.



Marginal effects on cases are in the left column. Marginal effects on deaths are in the right column.

Figure 3: Comparison of observed and predicted weekly cases assuming independent measurement errors.

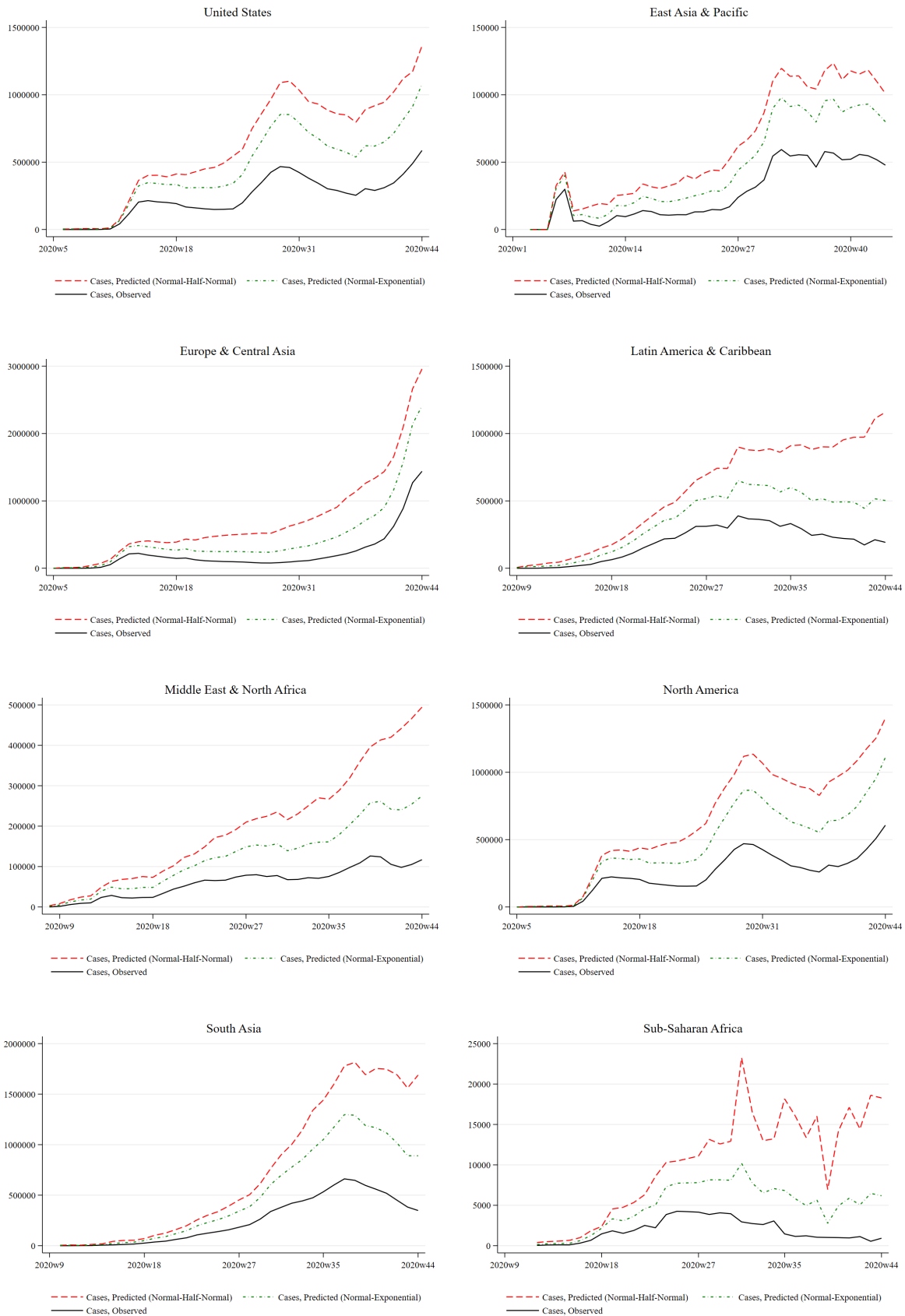


Figure 4: Comparison of observed and predicted weekly deaths assuming independent measurement errors.

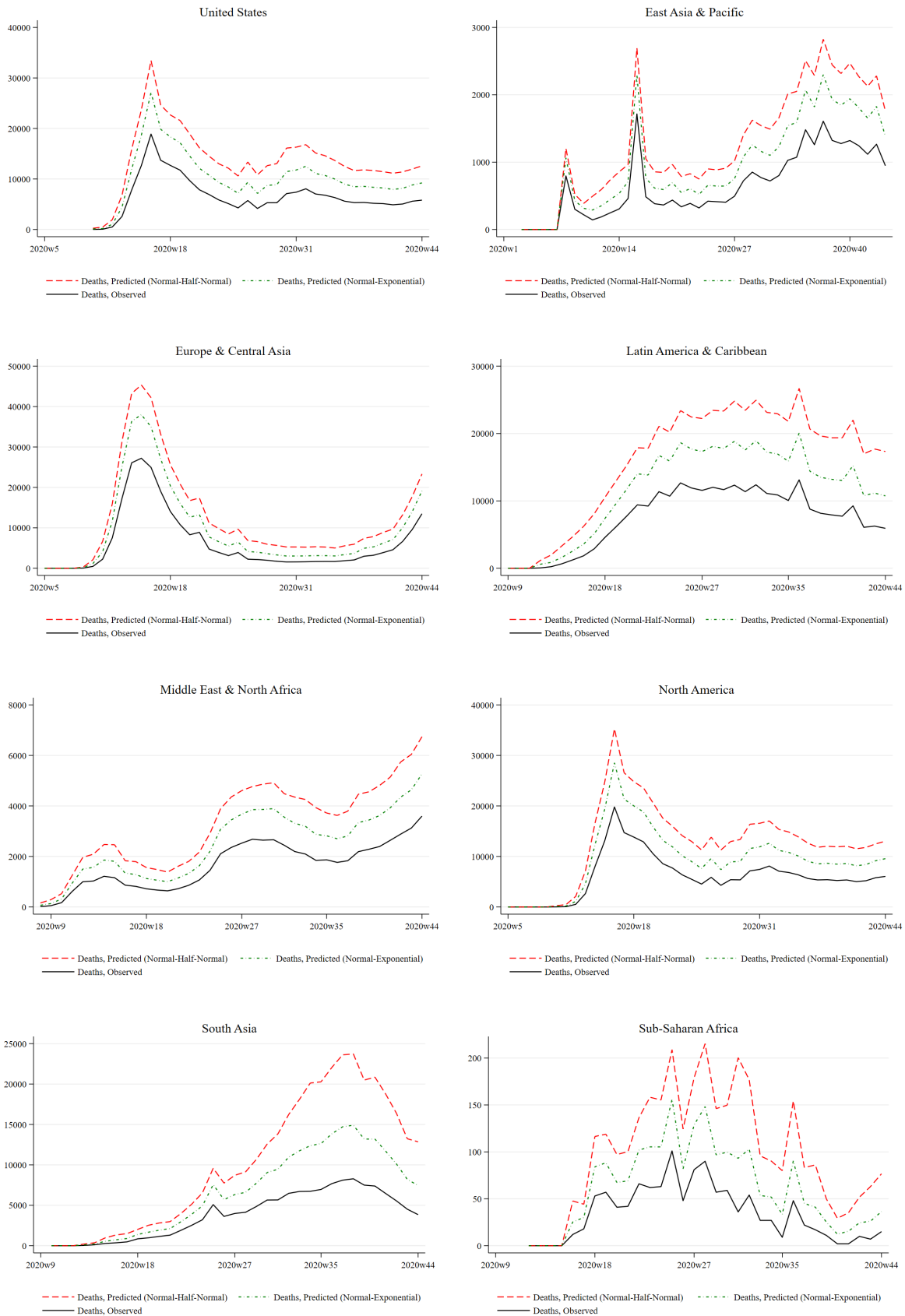


Figure 5: Comparison of observed and predicted weekly cases under the assumption of dependent measurement errors.

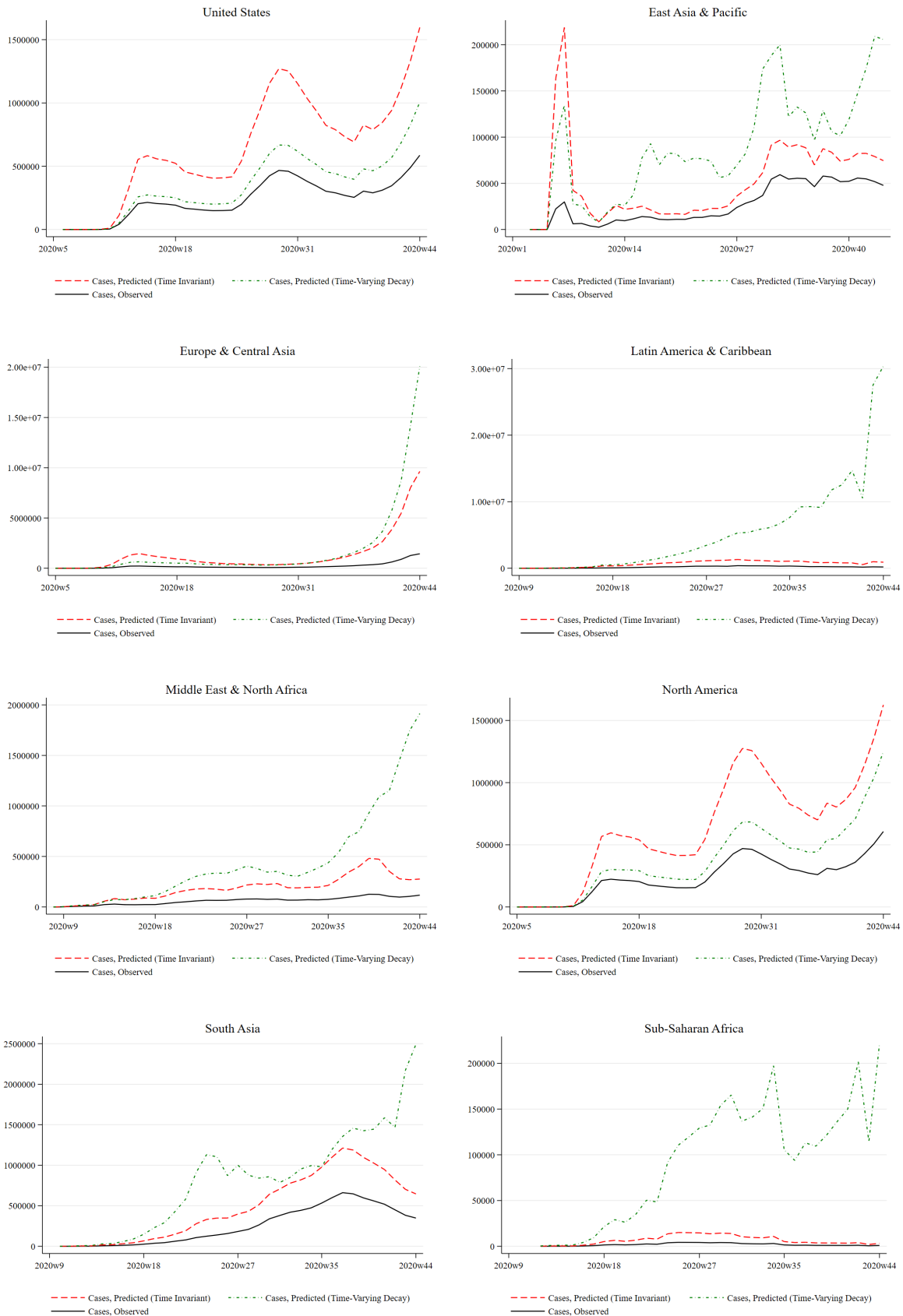


Figure 6: Comparison of observed and predicted weekly deaths under the assumption of dependent measurement errors.

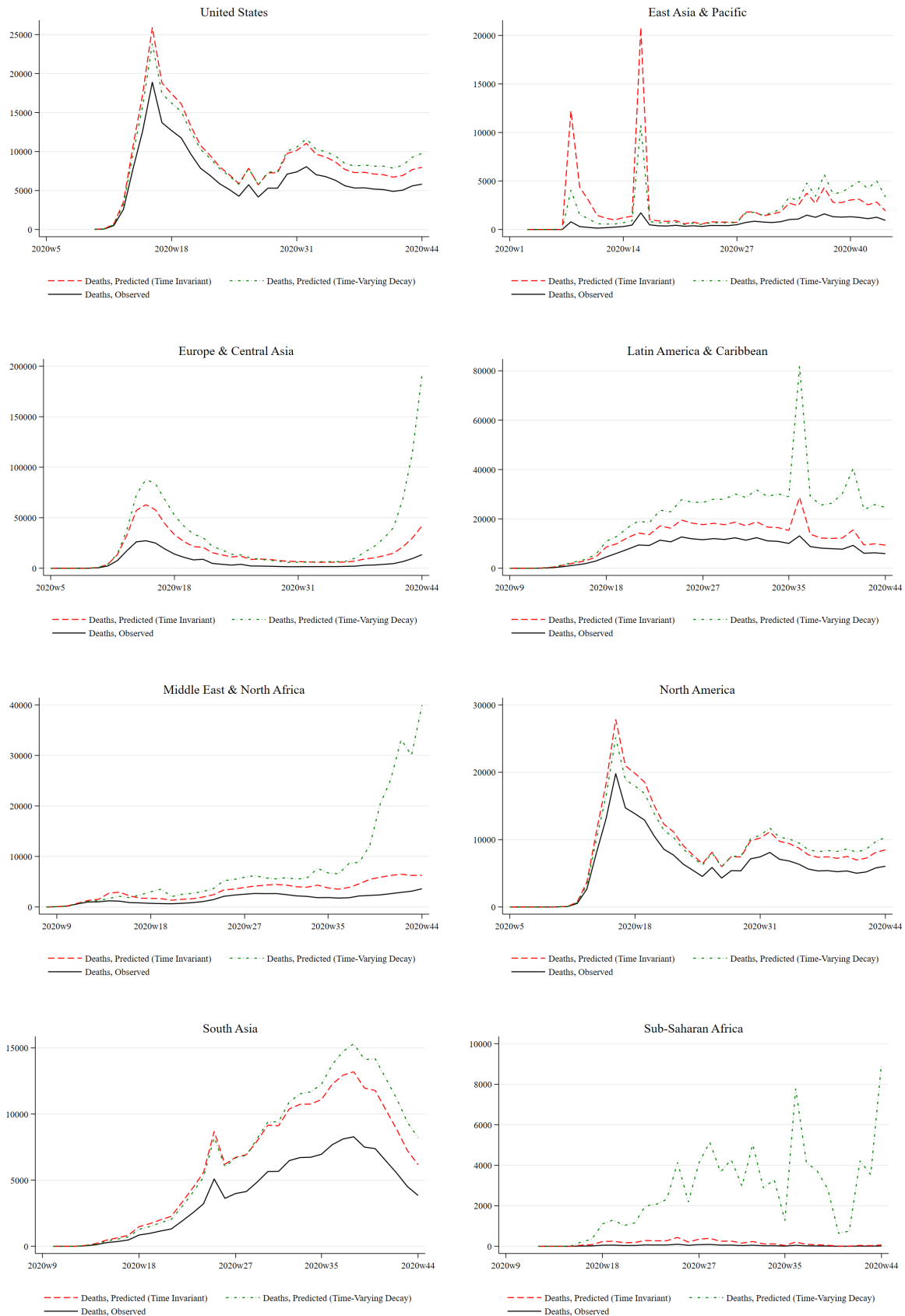


Figure 7: Comparison of the case fatality rate and infectious fatality rates obtained under different measurement error assumptions.



Case fatality rate is observed deaths one-week ahead divided by observed cases. Infectious fatality rate is predicted deaths one-week ahead divided by predicted cases.

Appendix A Supplemental Tables

Figure A1: Comparison of weekly multiplication factors for cases.

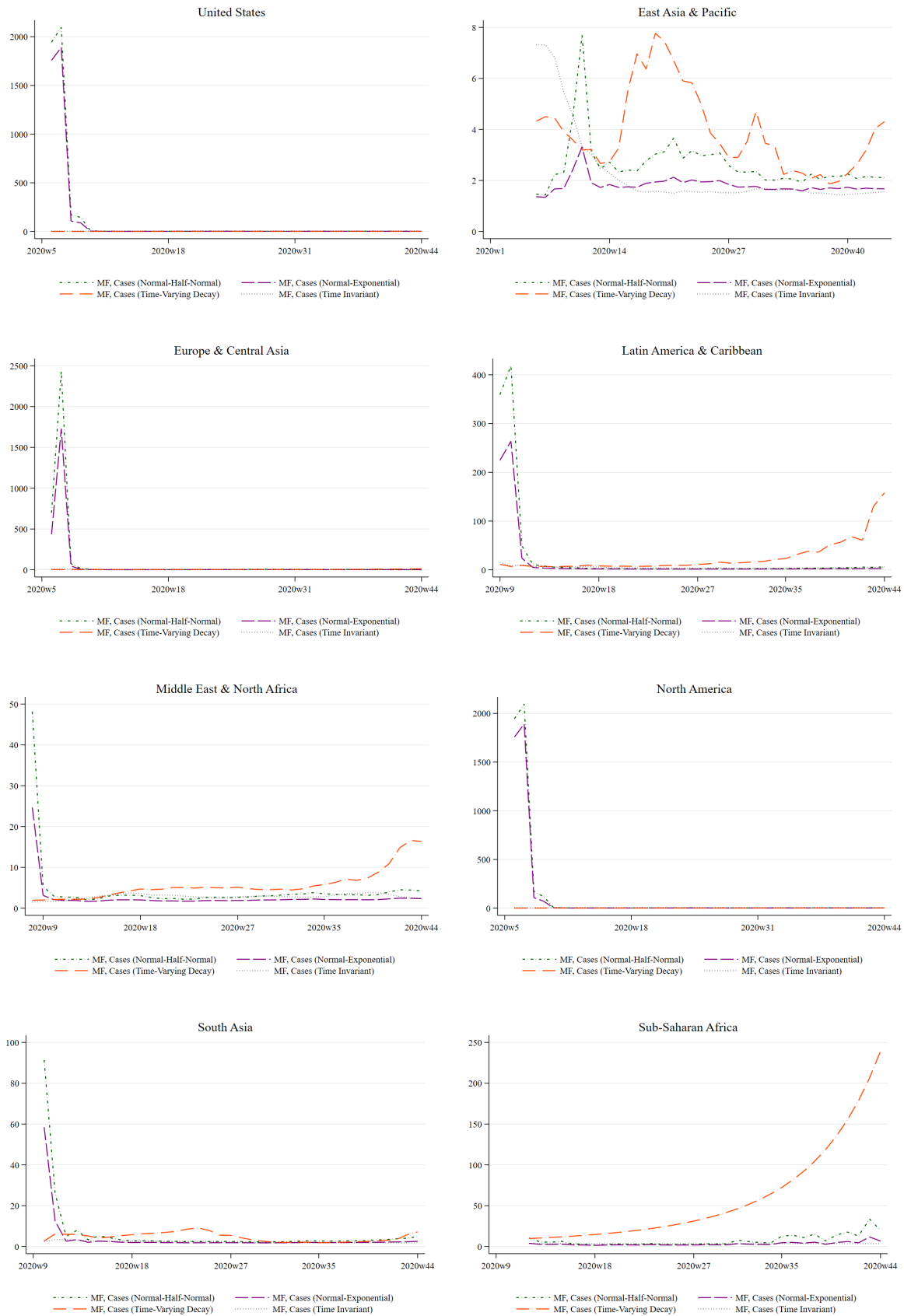


Figure A2: Comparison of weekly multiplication factors for deaths.

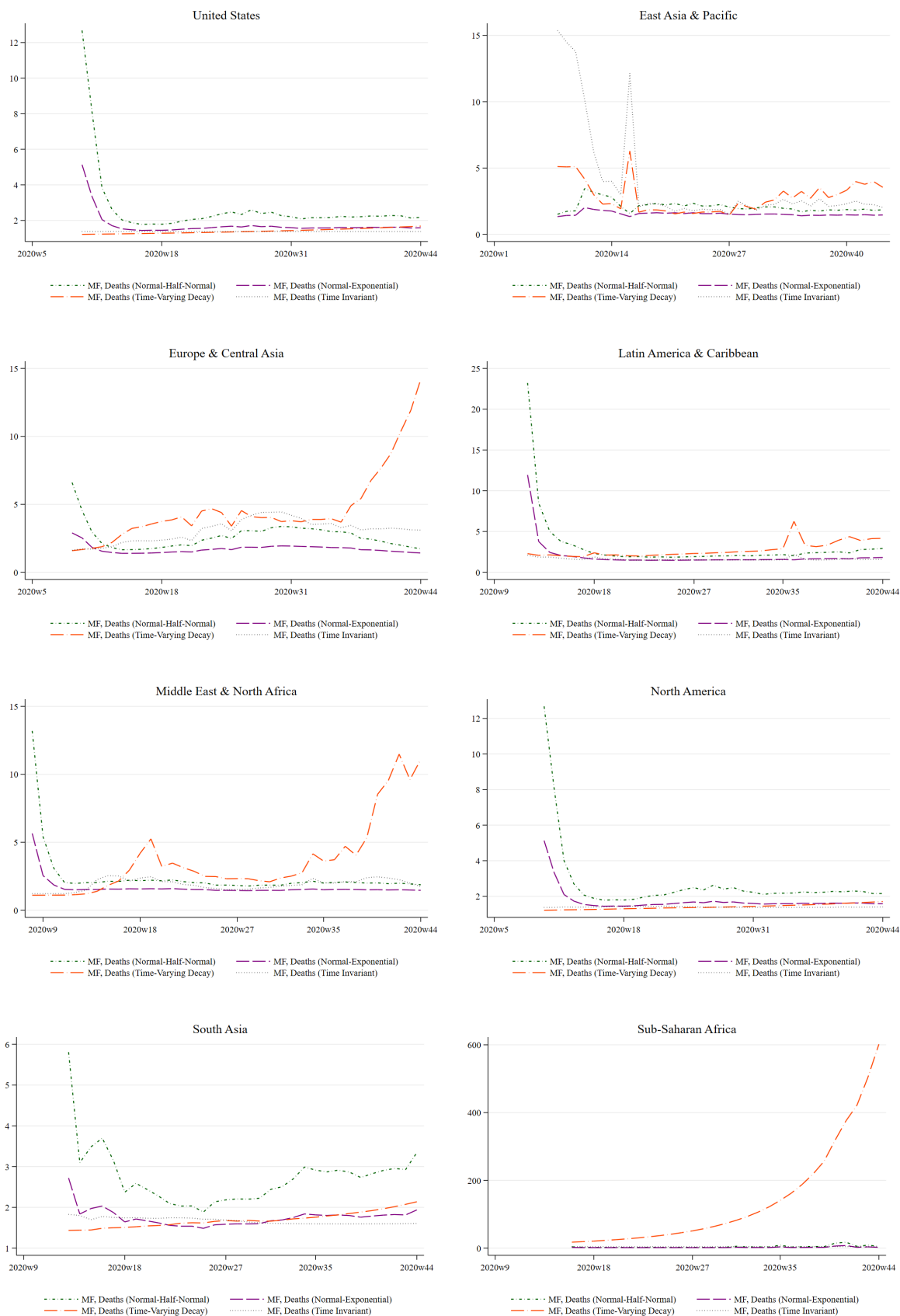


Figure A3: Estimated infection rates for select countries.

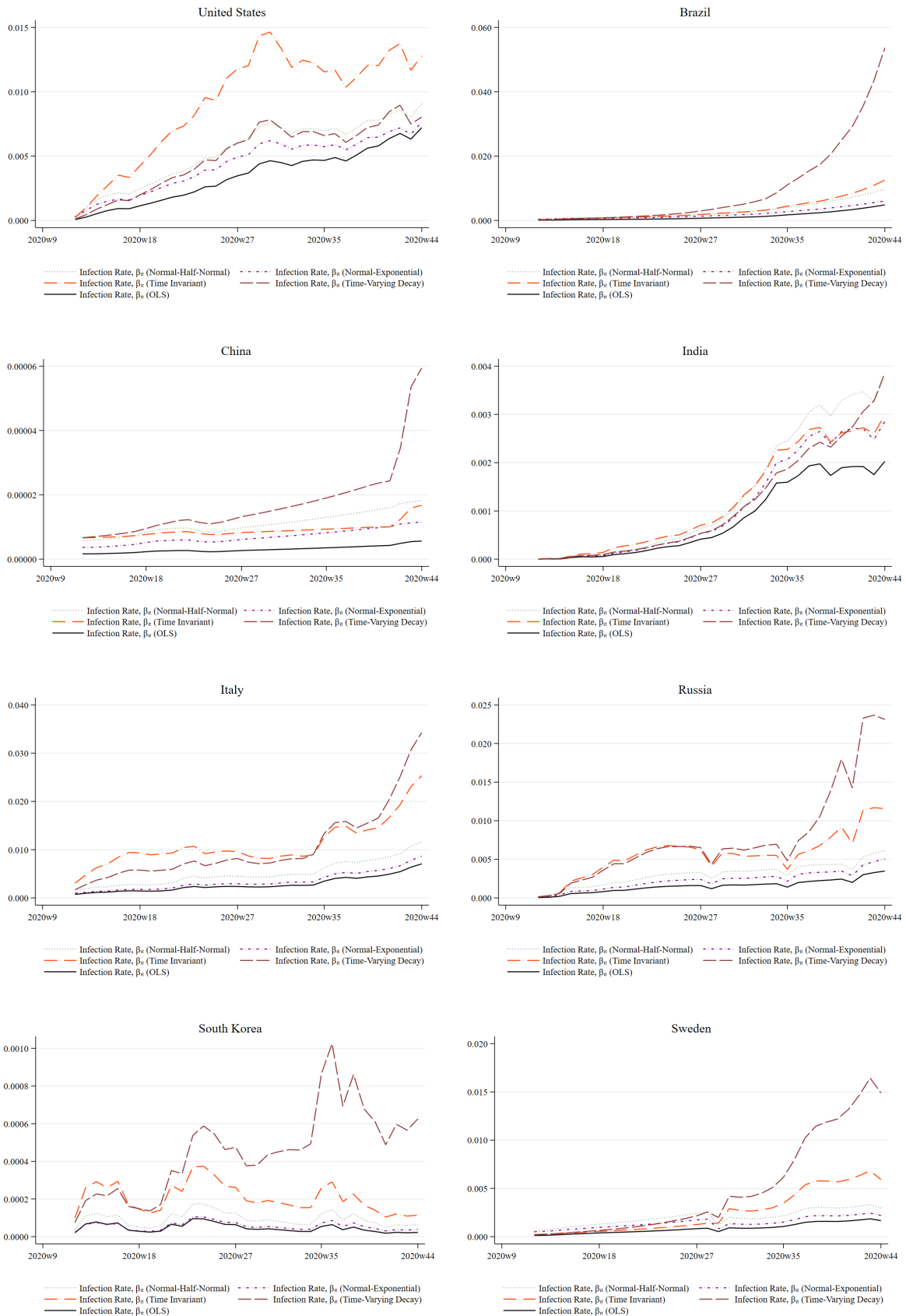


Figure A4: Estimated fatality rates for select countries.

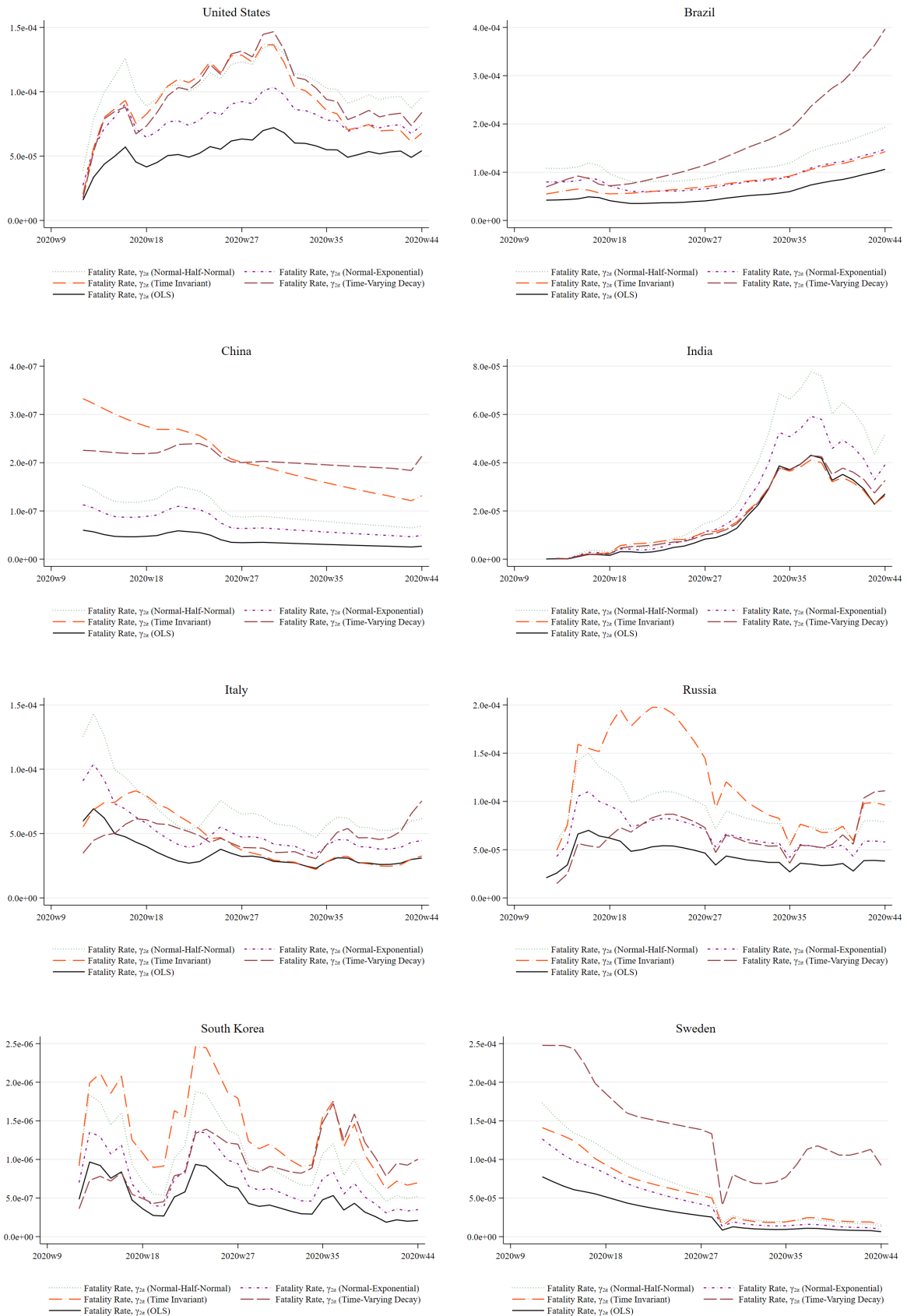


Figure A5: Estimated recovery rates for select countries.

